REPORT OF INVESTIGATIONS/1994

Field Test of an Alternative Longwall Gate Road Design

By Robert M. Cox, Thomas L. Vandergrift,
and John P. McDonnell

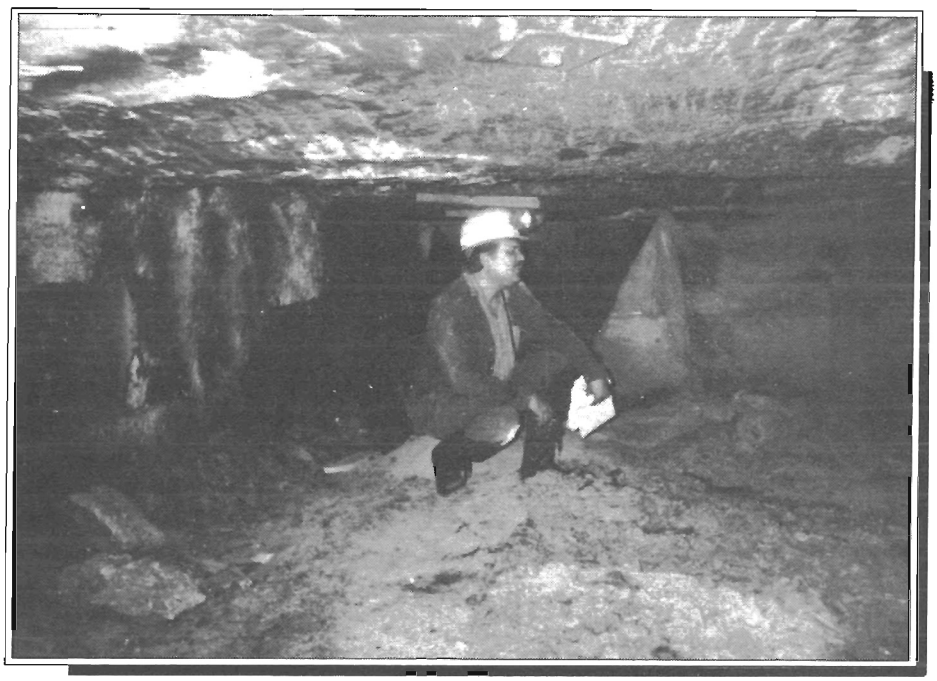

UNITED STATES DEPARTMENT OF THE INTERIOR

BUREAU OF MINES

U.S. Department of the Interior
Mission Statement

As the Nation's principal conservation agency, the Department of the Interior has responsibility for most of our nationally-owned public lands and natural resources. This includes fostering sound use of our land and water resources; protecting our fish, wildlife, and biological diversity; preserving the environmental and cultural values of our national parks and historical places; and providing for the enjoyment of life through outdoor recreation. The Department assesses our energy and mineral resources and works to ensure that their development is in the best interests of all our people by encouraging stewardship and citizen participation in their care. The Department also has a major responsibility for American Indian reservation communities and for people who live in island territories under U.S. administration.

Cover photograph: Assessment of gate road stability (photo by Robert Cox, Denver Research Center, Denver, CO).

Report of Investigations 9510

Field Test of an Alternative Longwall Gate Road Design

By Robert M. Cox, Thomas L. Vandergrift,
and John P. McDonnell

UNITED STATES DEPARTMENT OF THE INTERIOR
Bruce Babbitt, Secretary

BUREAU OF MINES

International Standard Serial Number
ISSN 1066-5552

CONTENTS

ILLUSTRATIONS

ILLUSTRATIONS—Continued

TABLES

UNIT OF MEASURE ABBREVIATIONS USED IN THIS REPORT

ft	foot	m	meter
MPa	megapascal	psi	pound per square inch

FIELD TEST OF AN ALTERNATIVE LONGWALL GATE ROAD DESIGN

By Robert M. Cox,[1] Thomas L. Vandergrift,[1] and John P. McDonnell[1]

ABSTRACT

The U. S. Bureau of Mines (USBM) MULSIM/NL modeling technique has been used to analyze anticipated stress distributions for a proposed alternative longwall gate road design for a western Colorado coal mine. The model analyses indicated that the alternative gate road design would reduce stresses in the tailgate entry without increasing stresses in the headgate entry. To test the validity of the alternative gate road design under actual mining conditions, a test section of the alternative system was incorporated into a subsequent set of gate roads developed at the mine.

The alternative gate road test section was instrumented with borehole pressure cells, as part of an ongoing USBM research project, to monitor ground pressure changes as longwall mining progressed. During the excavation of the adjacent longwall panels, the behavior of the alternative gate road system was monitored continuously using the USBM computer-assisted Ground Control Management System. During these field tests, the alternative gate road system was first monitored and evaluated as a headgate, and later monitored and evaluated as a tailgate. The results of the field tests confirmed the validity of using the MULSIM/NL modeling technique to evaluate mine designs.

[1]Mining engineer, Denver Research Center, U.S. Bureau of Mines, Denver, CO.

INTRODUCTION

The design and development of safe and stable longwall gate road systems are problems of paramount importance to the underground coal mining industry. Ensuring both the safety of longwall miners and the cost-efficient recovery of coal deposits depends on the ability of coal mining engineers to design and lay out gate road systems that will remain open during the high-speed mining of coal that is possible with today's mechanized longwall equipment. During the past decade, researchers at the U. S. Bureau of Mines (USBM) have been in the forefront in developing and testing innovative mine design and field monitoring tools as part of its mission to enhance mining safety and efficiency.

One of the most recent USBM developments is a nonlinear numerical modeling program called MULSIM NonLinear (MULSIM/NL) (*1*).[2] The program uses the displacement-discontinuity boundary-element approach in conjunction with nonlinear coal and gob properties to simulate ground stresses for a given mine layout. MULSIM/NL provides mining engineers with a valuable design tool for projecting anticipated ground stress and displacement patterns for different longwall mine layouts. Thus the design engineer can analyze and test the merits of alternative longwall gate road systems from a ground control perspective.

Another recent USBM development is a computerized Ground Control Management System (GCMS) that is currently being field tested at a longwall coal mine in western Colorado (*2-4*). The GCMS continuously monitors ground response to the high-speed extraction of longwall panels, and displays data such as shield loads and ground pressures in real time. The GCMS also processes and stores the data, and can be used to create graphic displays for the real-time examination of ground conditions and the historical trend analysis of the rock mechanics data for design purposes.

As part of ongoing research efforts, the USBM has been investigating the design and stability of gate road systems at the test mine using the GCMS. Mine observations and analyses of the ground response data monitored at the mine during the excavation of the first two longwall panels suggested that the design and layout of the existing gate road system might be a contributing factor to the instability of the tailgate roadways (e.g., floor bumps, pillar sloughage, and roof-cutter failures). Thus, mine management decided that a reversal of the existing gate road pillar arrangement might improve tailgate roadway stability.

In a cooperative research effort between the USBM and mine management, a gate road test section incorporating the alternative system pattern was developed, and the pillars were instrumented with borehole pressure cells (BPCs) to monitor gate road ground pressure changes. A study of the proposed alternative gate road system was also initiated using the MULSIM/NL modeling technique. During the subsequent mining of panels 4 and 5, the ground loading behavior of the gate road pillars within the test section was monitored using the GCMS, and the resulting field data compared with the predictive model analyses. The alternative gate road system was first monitored and evaluated as a headgate pillar system during the mining of panel 4, and then monitored and evaluated as a tailgate pillar system during the mining of panel 5.

FIELD SITE DESCRIPTION

The test site is located in a western Colorado coal mine that produces steam coal from the Wadge Seam. The mine uses a high-speed mechanized longwall system designed to extract coal in a series of longwall panels that are progressively being mined up dip in a west to east direction as shown in figure 1.

MINE LAYOUT AND GEOLOGY

The Wadge Coal Seam in the test site area is about 3 m (10 ft) thick, strikes N. 50 E., and dips about 8% to the northwest. The longwall panels lie beneath about 340 m (1,100 ft) of overburden composed of interbedded shales and sandstones. The longwall panels are oriented at an approximate angle of 55° to the regional geologic structure, and the mine area is bounded to the northwest by a northeast-trending thrust fault, and to the east by the north-south-trending Oak Creek Anticline. The face cleats in the coal seam strike about N. 50 W., approximately parallel to the prominent joint set that occurs throughout the mine area. Several joint-shear zones oriented about N. 60 W. dissect the mine area, and one strike-slip fault oriented about N. 30 W. occurs in the eastern end of the longwall panels as shown in figure 1.

The typical stratigraphy of the strata enclosing the coal seam in the vicinity of the longwall panels is shown in the geophysical log in figure 2. The immediate roof above the longwall panels is composed of interbedded shales and sandstones (Beds A and B) that vary in total thickness

[2]Italic numbers in parentheses refer to items in the list of references preceding the appendixes.

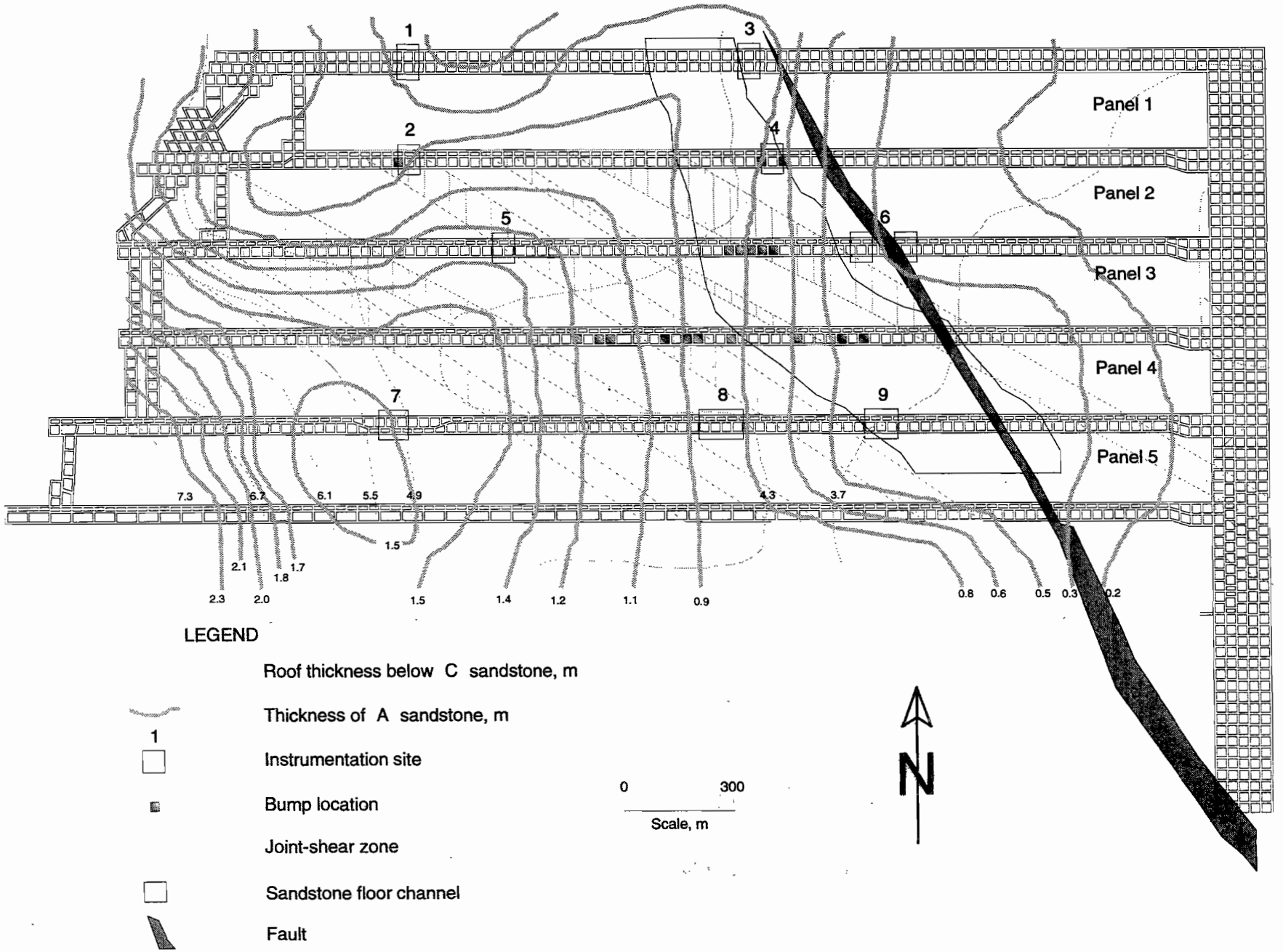

Figure 1.—Mine map showing geologic structure and locations of instrumented test sites.

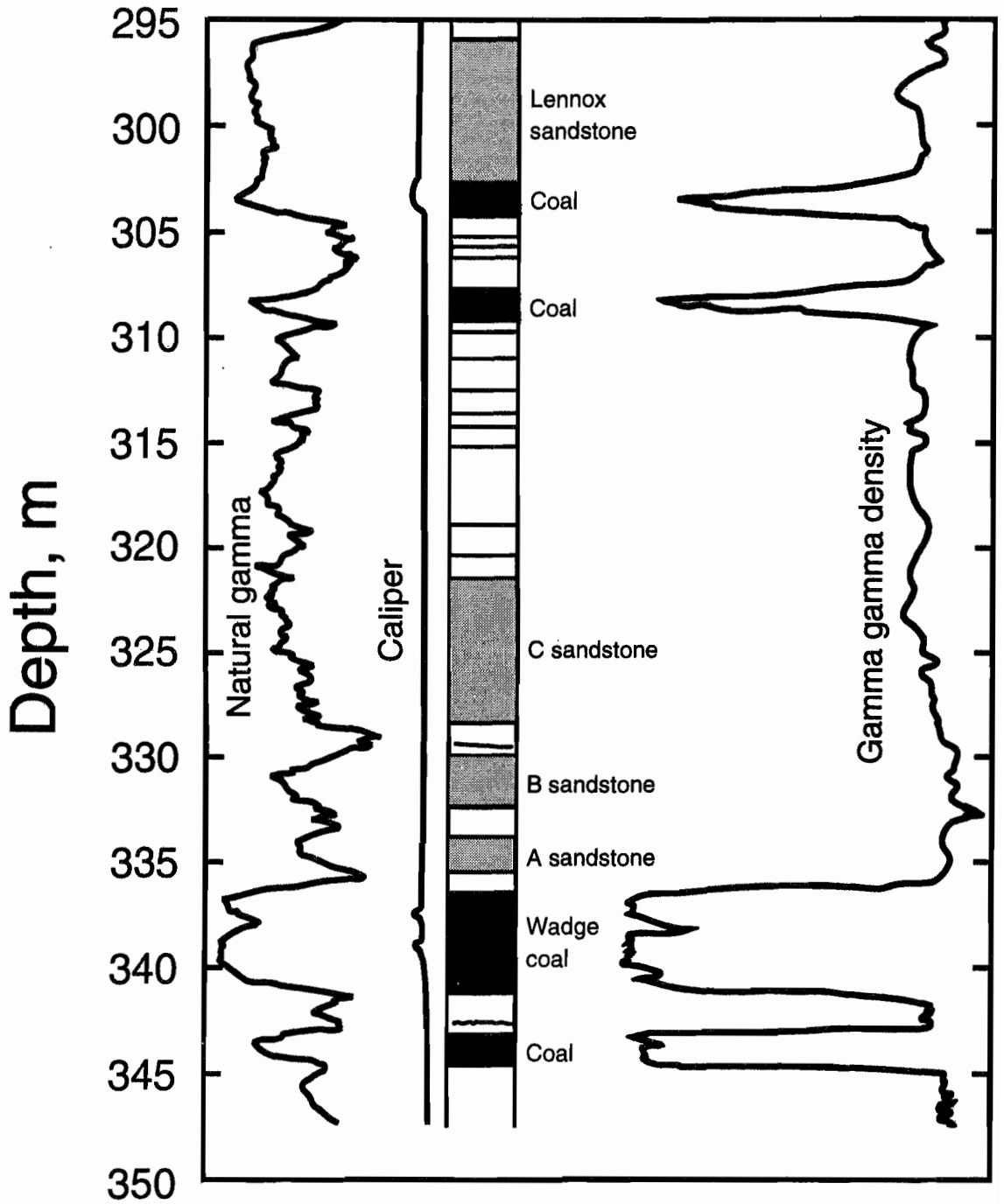

Figure 2.—Stratigraphy of mine area.

from 3 to 6 m (10 to 20 ft) going from east to west across the panels. The main roof above the panels is composed of a sandstone unit (Bed C) that varies in thickness from 5 to 8 m (16 to 26 ft) going from east to west across the panels. Isopacs of the thickness of the A sandstone and the immediate roof (A and B) are shown in figure 1. The relative thickness of these units is believed to be related to the location and occurrence of tailgate floor bumps.

The Lennox Sandstone Unit, which is about 4 m (13 ft) thick, occurs about 21 m (70 ft) above the Wadge Coal Seam and is underlain by two thin coal seams. The Twenty-Mile Sandstone Unit that forms the prominent bluffs in the region occurs about 210 m (700 ft) above the longwall panels. The intervening strata between these massive sandstones are composed of interbedded shales and siltstones.

The immediate floor of the Wadge Seam is composed of carbonaceous shales and interbedded sandstones underlain by a weaker zone consisting of either a thin leader of coal and/or weak shale bed as shown in figure 2. The approximate location of this weak zone of coal and/or shale beneath a relatively strong immediate floor is conducive to brittle fracture and dynamic heave of the floor (i.e., floor bumps) when the tailgate roadway is subjected to the elevated abutment pressures created by longwall mining. A sandstone floor channel occurs immediately west of the strike-slip fault zone as shown in figure 1. This structure may also be related to floor bump problems in the tailgate roadways.

GEOMECHANICAL DATA

Slickensided surfaces along the joints and bedding plane surfaces within the shale contact between the coal seam and the enclosing sandstones indicate strike-slip movements roughly parallel to the dip of the coal seam in a northwest direction. The orientation and magnitude of the in situ stress field used in the model analysis was approximated from a consideration of the overburden pressure and the structural geology of the mine area to be:

Maximum Principal Stress = 13 MPa (1,875 psi), N. 35 W.,

Intermediate Principal Stress = 9 MPa (1,250 psi), N. 55 E., and

Minimum Principal Stress = 9 MPa (1,250 psi), vertical.

The longwall abutment pressures and the orientation of the longwall panels at an approximate angle of 55° to the direction of the maximum principal stress would be expected to increase the magnitude of vertical and horizontal stress concentrations in the tailgate end of the retreating longwall faces. These stress concentrations would be expected to cause ground control problems such as the tailgate floor bumps that have been observed during the extraction of the first three panels.

A review of the rock mechanics data provided by the mining company, tempered with field observations and experience, suggests that for practical design purposes the typical rock strength characteristics contained in table 1 might be used.

Table 1.—Mine rock strength characteristics

Rock type	In situ strength		Modulus of elasticity	
	MPa	psi	MPa	psi
Coal	31	4,500	2,750	4×10^5
Mudstones	14	2,000	5,200	7.5×10^5
Sandstones . . .	83	12,000	10,350	1.5×10^6
Shales	41	6,000	6,900	10^6

EXISTING GATE ROAD DESIGN

In the existing mine plan, longwall panels are being developed about 195 m (640 ft) wide by 2,750 m (10,000 ft) long using a three-entry gate road system composed of 6-m (20-ft) roadways, one small pillar (about 10 m (35 ft) wide and 24 m (80 ft) long) adjacent to the headgate, and one large pillar (about 24 m (80 ft) squared) adjacent to the tailgate (see figure 1). Alternating crosscuts are driven on about 30-m (100-ft) centers, creating three-way intersections for improved roof stability. For location and reference purposes, the gate road entries are numbered 1 to 3 from south to north; No. 1 entry being the tailgate roadway of each successive longwall panel, and No. 3 being the headgate (beltway) of each longwall panel.

Field observations indicated that as longwall panels 2, 3, and 4 were mined, the small pillars located adjacent to the headgate failed about 40 m (125 ft) behind the face and transferred the side abutment pressures onto the larger pillars left to protect the tailgate of the next panel. The increased side abutment pressures being carried by the larger pillars, acting in conjunction with the frontal abutment pressures created by the extraction of the active longwall panel, are believed to be responsible for the increased ground control problems encountered in the tailgate roadways of each successive panel. These tailgate ground control problems are manifested primarily as excessive tailgate floor heave (greater than 0.3 m (1 ft)) and occasional tailgate floor bumps that damage roadway supports up to 30 m (100 ft) outby the operating face.

Thus it was concluded that the existing design of the gate road pillar system might be a contributing factor to tailgate roadway instability. A reversal of the position of the small pillar and the large pillar in the gate road layout was proposed as a possible practical remedy to the existing tailgate ground control problems.

ALTERNATIVE GATE ROAD DESIGN TEST SITE

To test the validity of an alternative gate road design under actual mining conditions, a test section of the reversed pillar arrangement was incorporated in a subsequent set of gate roads developed at the mine. During the development of the headgate roadway system for panel 4, a test section was mined in which the positions of the small pillar and the large pillar were reversed (see instrument site 7, figure 1).

After the development of the panel 4 gate road test site, several model analyses of the alternative gate road layout were conducted using the USBM's new MULSIM/NL modeling program. These model analyses indicated that stress conditions in the tailgate might be improved with a reversal of the positions of the gate road pillars.

The alternative test site consisted of a three-entry system composed of 5.5-m (18-ft) roadways, a series of large pillars about 27 m (90 ft) wide by 24 m (80 ft) long located adjacent to the headgate, and smaller pillars about 9 m (30 ft) wide by 24 m (80 ft) long located adjacent to the tailgate. The test site pillars were instrumented with BPC to monitor vertical stress changes during the mining of panels 4 and 5 adjacent to the test section as shown in figure 3. The alternative gate road system was first monitored and evaluated as a headgate entry, and then monitored and evaluated as a tailgate roadway.

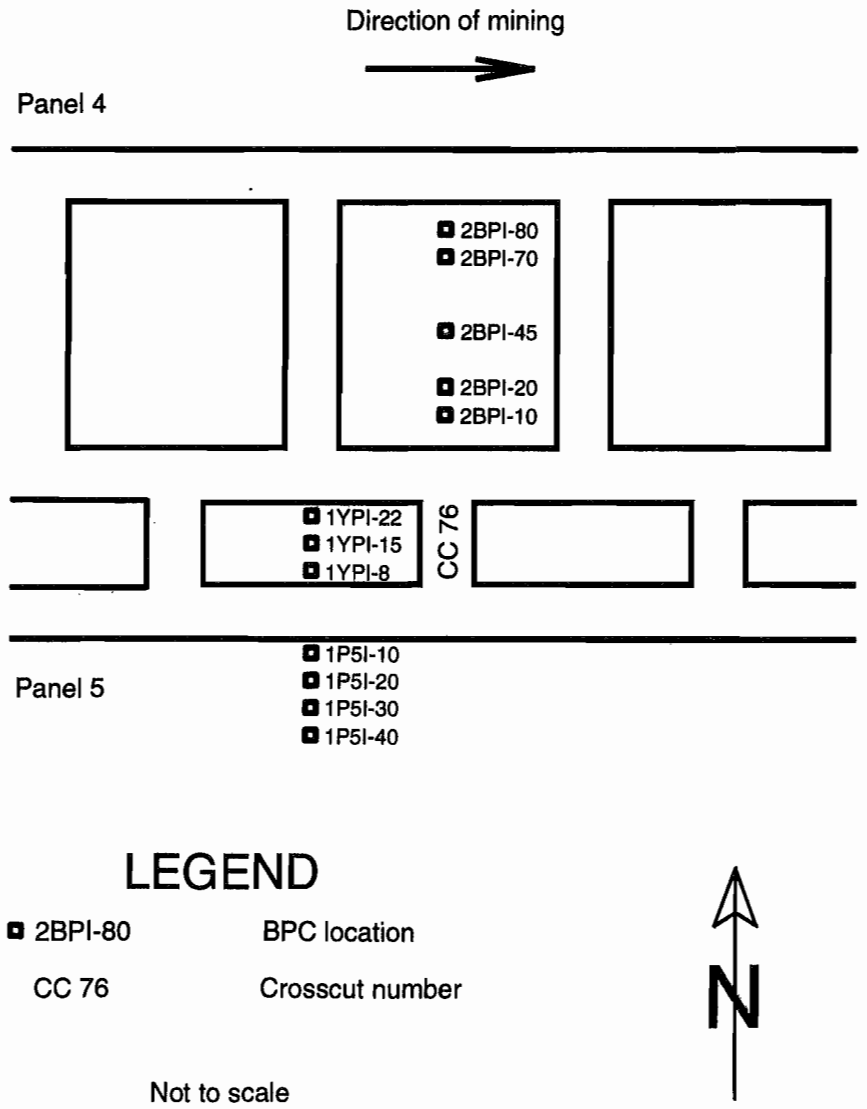

Figure 3.—Location and position of BPCs at alternative gate road test site.

NUMERICAL MODELS

Numerical models of the exact layout and conditions of longwall panels using both the existing mine layout and the alternative gate road systems were formulated and analyzed using the USBM's nonlinear boundary-element program MULSIM/NL (see figures 4 and 5). The resulting analyses indicated that the alternative gate road design might improve tailgate conditions without deteriorating headgate conditions. Subsequently, models of the exact layout of the alternative gate road test site were analyzed to provide data for comparison with the field ground pressure measurements monitored during the mining of panels 4 and 5 adjacent to the test site (see figure 5*C*).

MULSIM/NL MODELING METHODS

MULSIM/NL is a three-dimensional boundary-element method computer program recently developed by the USBM for stress analysis of complex coal mine layouts. The program is easily learned, simple to use, and can be run on a personal computer. It is a very effective design tool for quantifying the effects of changes in mine geometries and coal seam properties. The program computes stress and displacements within the coal seam horizon, and can be used to conduct realistic stress analyses of complex longwall gate road systems. Thus, the coal mine design engineer can easily compare alternative mine layouts, and avoid costly surprises and design modifications after mining commences.

The creation of a MULSIM/NL model involves three major steps: (1) definition of model parameters; (2) input of the mining geometry; and (3) selection of coal seam material properties. Input to the program is relatively simple. The input file consists of three sections: (1) the control section that defines basic parameters, such as the

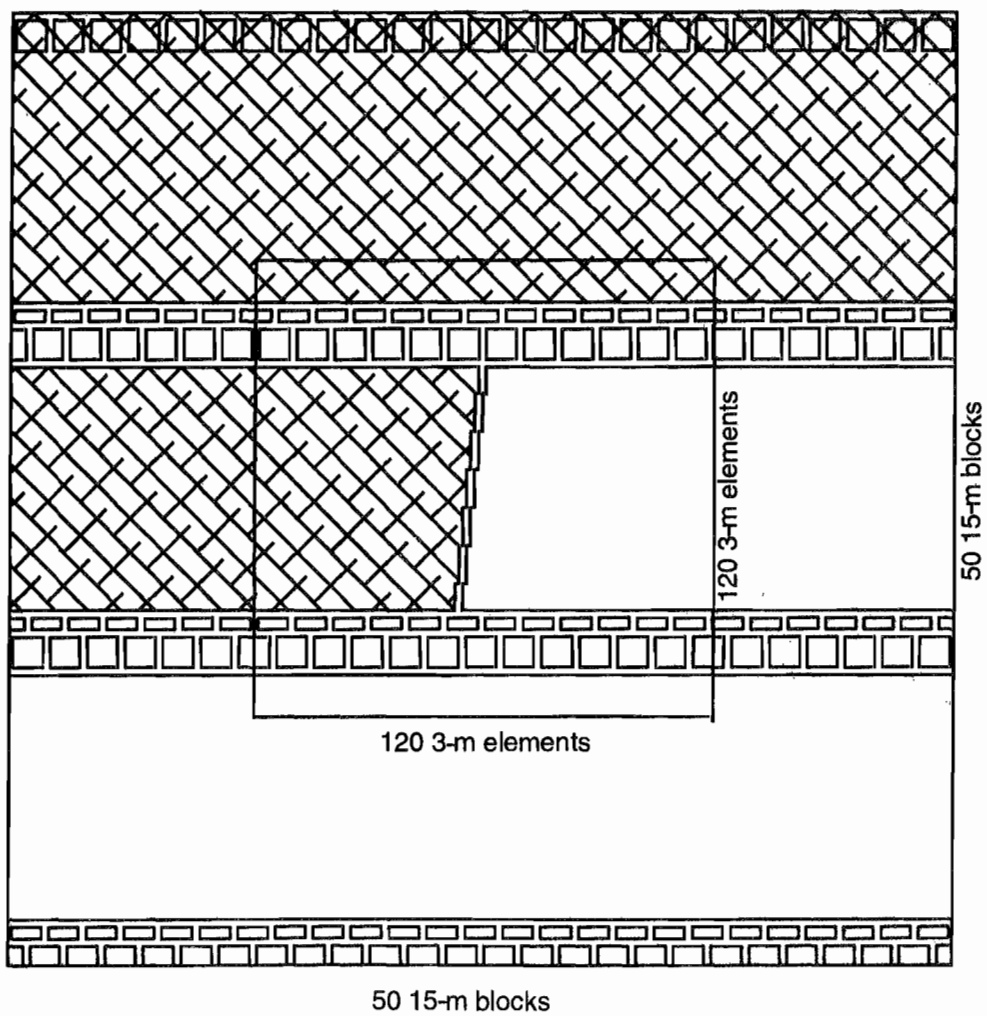

Figure 4.—Basic geometric parameters of MULSIM/NL models.

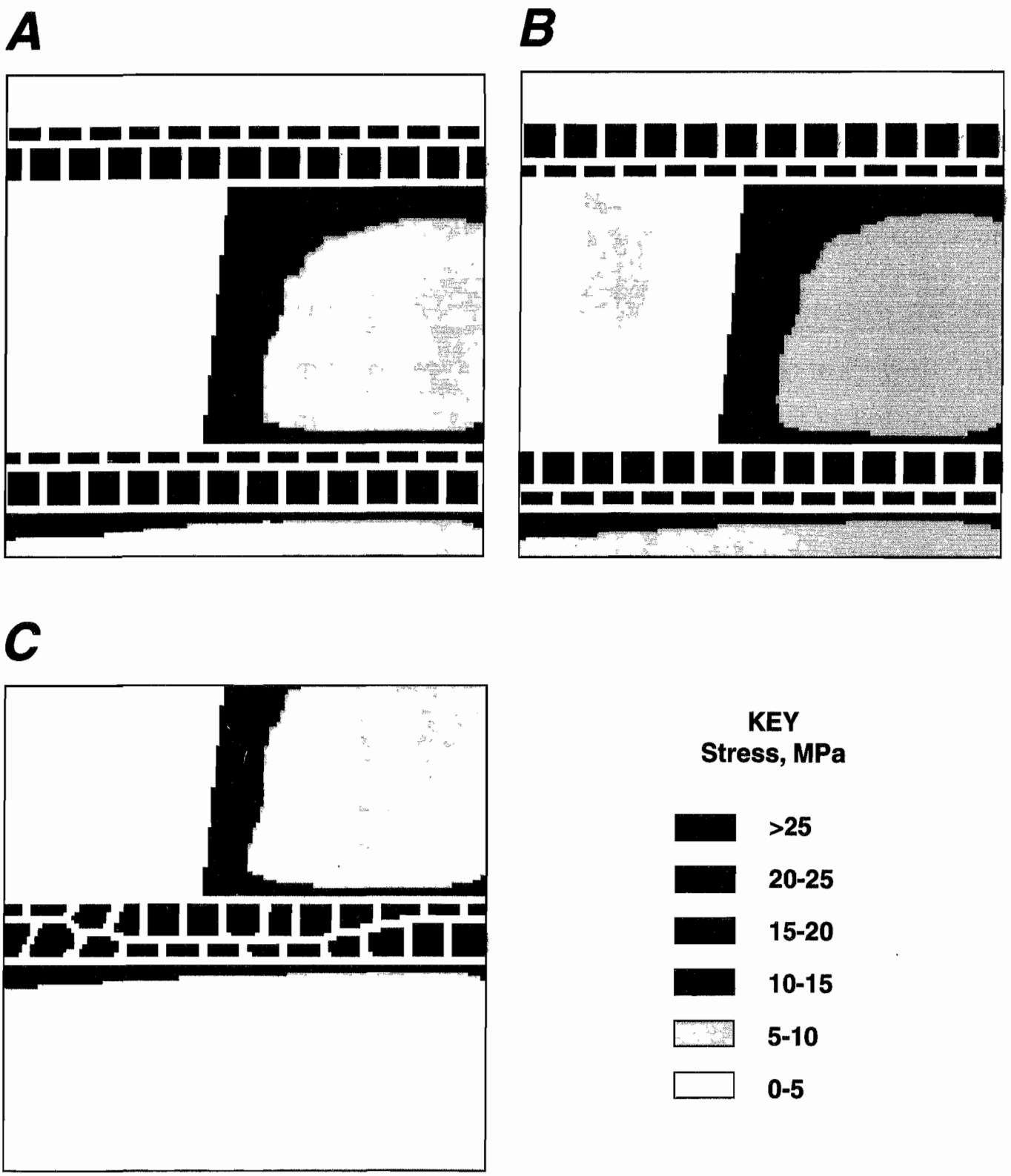

Figure 5.—MULSIM/NL stress pattern of existing, proposed, and field test site gate road systems.

model size, the physical characteristics of the enclosing rock mass, the in situ stress field, and the depth of mining; (2) the fine-mesh section that defines the detailed geometry of the modeled mine layout; and (3) the coarse-element mesh that defines the enclosing model geometry of the mine layout. Both the fine and coarse meshes are used to define the coal seam material properties. Within each mesh, individual elements are defined in terms of their stress-strain behavior.

Figure 4 indicates the basic geometric model parameters used in these model analyses; a 50 by 50 grid of 15-m (50-ft) coarse-mesh blocks enclosing a 120 by 120 grid of 3-m (10-ft) fine-mesh elements. The mine geometry was laid within the fine-mesh model as closely as possible to the existing mine geometry of 6-m (20-ft) entries, 9-m by 24-m (30-ft by 80-ft) small pillars, and 24-m (80-ft) square large pillars. The longwall face area was modeled 6 m (20 ft) wide to realistically accommodate the presence of the longwall mining machinery.

Based on a review of the rock mechanics data base provided by the mine operator, tempered with field observations and experience, the authors selected the basic input material properties presented in table 2 for the model analyses.

Table 2.—Material properties for numerical models

Seam thickness, m (ft)	3	(10)
Depth of mine, m (ft)	335	(1,100)
Modulus, MPa (psi):		
Coal seam	2,750	(4.0×10^5)
Gob material	275	(4.0×10^4)
Rock strata	8,275	(1.2×10^6)

Appendix A contains a printout of a typical computer input used in this study to demonstrate the steps involved in the formulation of a MULSIM/NL model.

SELECTION OF COAL-ELEMENT PROPERTIES

The distinguishing feature of MULSIM/NL is its nonlinear material model elements that provide the ability to simulate nonlinear behavior of coal as it loads and fails as observed in the mine and the laboratory. Of the three coal-element models available in the USBM MULSIM/NL program, the strain-softening model element is the most useful for coal mine design work, since it simulates the typical peak strength and residual loading characteristics of coal. The required input parameters for the strain-softening model element are the peak stress, the peak strain, the residual stress, the residual strain, and Poisson's ratio (see figure 6). This model dictates that stress

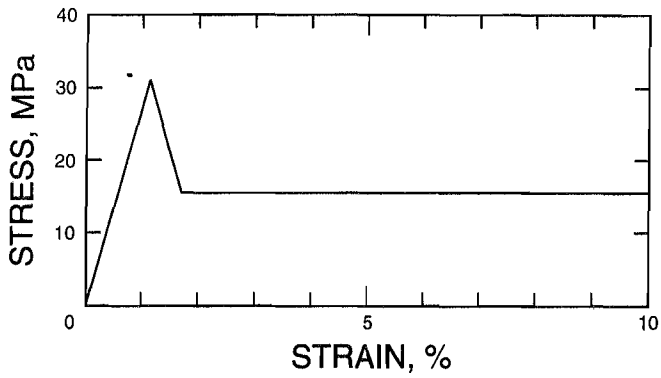

Figure 6.—Strain-softening characteristics of coal elements, Model A analyses.

remains constant beyond the residual strain level. Therefore, by inputting the peak and residual stresses and strains, the complete stress-strain behavior of this coal element is defined.

The key to formulating realistic mine models of longwall stress distributions lies in the proper choice and arrangement of coal-seam-material elements within the MULSIM/NL model. In this study, two methods were used to select coal model elements: a practical approach designated as Model A analyses, and an empirical approach designated as Model B analyses.

Model A Analyses

The Model A analyses were formulated using the mine rock strength characteristics listed in table 1. Based on field observations and engineering experience concerning the design and layout of coal mine openings, the residual strength of the coal was assumed to be approximately 50% of the peak strength; thus yielding input-element properties of the coal strength as shown in figure 6 and listed in table 3.

Table 3.—Strain-softening coal characteristics

	MPa	psi
Seam modulus	2,750	4.0×10^5
Residual strength	15.5	2,250
Yield strength	31	4,500

These coal-element properties were used to formulate the initial model analyses of the existing gate road system and the alternative gate road design. In addition, the

panel gob was modeled using a linear-elastic element with a modulus of 275 MPa (4.0×10^4 psi).

Figure 5*A* is a plot of the ground stress patterns resulting from the Model A analysis of the existing longwall face and gate road system. The results show the development of the abutment pressure zone ahead of and adjacent to the excavated longwall panels and the complete yielding of the tailgate pillars inby the face. Note that the smaller headgate pillar begins to yield about one crosscut inby the face and completely yields within two crosscuts inby the face. The results also indicate that the yielding of the small headgate pillar causes the high stress pressure abutment created by the excavated panel to form along the inby side of the large-pillar line adjacent to the tailgate roadway of the next panel to be mined. The location of this zone of high stress concentration corresponds with the location of the poor ground control problems observed in the tailgate roadways of the existing gate road system.

Figure 5*B* is a plot of the stress patterns resulting from the Model A analysis of the proposed alternative gate road layout that reverses the positions of the small pillar and the large pillar. In general, the results indicate a more favorable distribution of ground pressures around the longwall panels. The resulting stress pattern of the alternative gate road layout indicates that the gob side (about 3 m (10 ft)) of the large pillar does not begin to yield until the face has advanced about 60 m (200 ft) beyond a given pillar, and that the high stress abutment zone created by the excavated panel is confined to the interior portions of the large pillar. The large pillars thus provide a stronger support structure for the tailgate of the next panel. The results also indicate that the large pillars, when placed adjacent to the headgate, provide greater protection to the headgate roadway (i.e., lower stress concentrations along the belt conveyor roadway). The relocation of the large pillars also protects the small pillars from excessive abutment loading after extraction of the first panel (i.e., lower stress concentrations along the tailgate roadway of the next panel).

These model analyses suggested that the tailgate roadway ground conditions, under existing conditions, might be improved using the new alternative gate road system.

Model B Analyses

The Model B analyses were developed as a second approach to the selection of material properties for coal-model elements. This approach was based on a study of coal pillar pressure responses monitored using BPCs during the mining of longwall panels 1, 2, and 3. After performing a detailed analysis of the BPC data from five instrumented gate road sites in the test mine, three different coal material models were created for this study as shown in figure 7. Each of the coal elements has an initial modulus of 3,450 MPa (500,000 psi). The unconfined coal-model element, representing any coal structure within 3 m (10 ft) of an underground opening, yields at 31 MPa (4,500 psi) and has a residual strength of 16.6 MPa (2,400 psi). The small-pillar core-model element, representing moderately confined coal structure, has a yield strength of 41 MPa (6,000 psi) and a residual strength of 27.5 MPa (4,000 psi). The confined coal structures, within the large pillars and the panel abutment zones, are modeled to have a peak strength of 48 MPa (7,000 psi) that slowly yields to a residual strength of 24 MPa (3,500 psi). In addition, a strain-hardening gob-model element was used that allows the modeled gob material to stiffen as it strains (see figure 7). Based on data published by Peng (*5*), this model was given an initial modulus of 103 MPa (15,000 psi) and a final modulus of 345 MPa (50,000 psi). These material elements, as previously described, were used to formulate Model B analyses of the alternative gate road test section.

A review of the results of Model A and B analyses, in combination with an analysis of BPC field data from the test section, has provided USBM researchers with the opportunity to judge the value of MULSIM/NL as a design tool, and evaluate the performance of the new gate road design under actual mining conditions.

COMPARISON OF GATE ROAD MODELS

Comparisons of the resulting stress patterns for Model A and Model B analyses of alternative gate road test section are shown in figure 8. The two methods of selecting coal element properties yield similar stress patterns, and both support the conclusion that the alternative gate road design would improve gate road ground conditions. The only differences are that Model B indicates higher abutment pressures ahead of the longwall face, and higher estimates of loading in the gate road pillars after mining of the longwall panels. Otherwise the location of the pressure abutment and general stress pattern to be expected remains about the same for the two models. The details of the input data for each of the alternative gate road test site MULSIM/NL models are presented in appendix B.

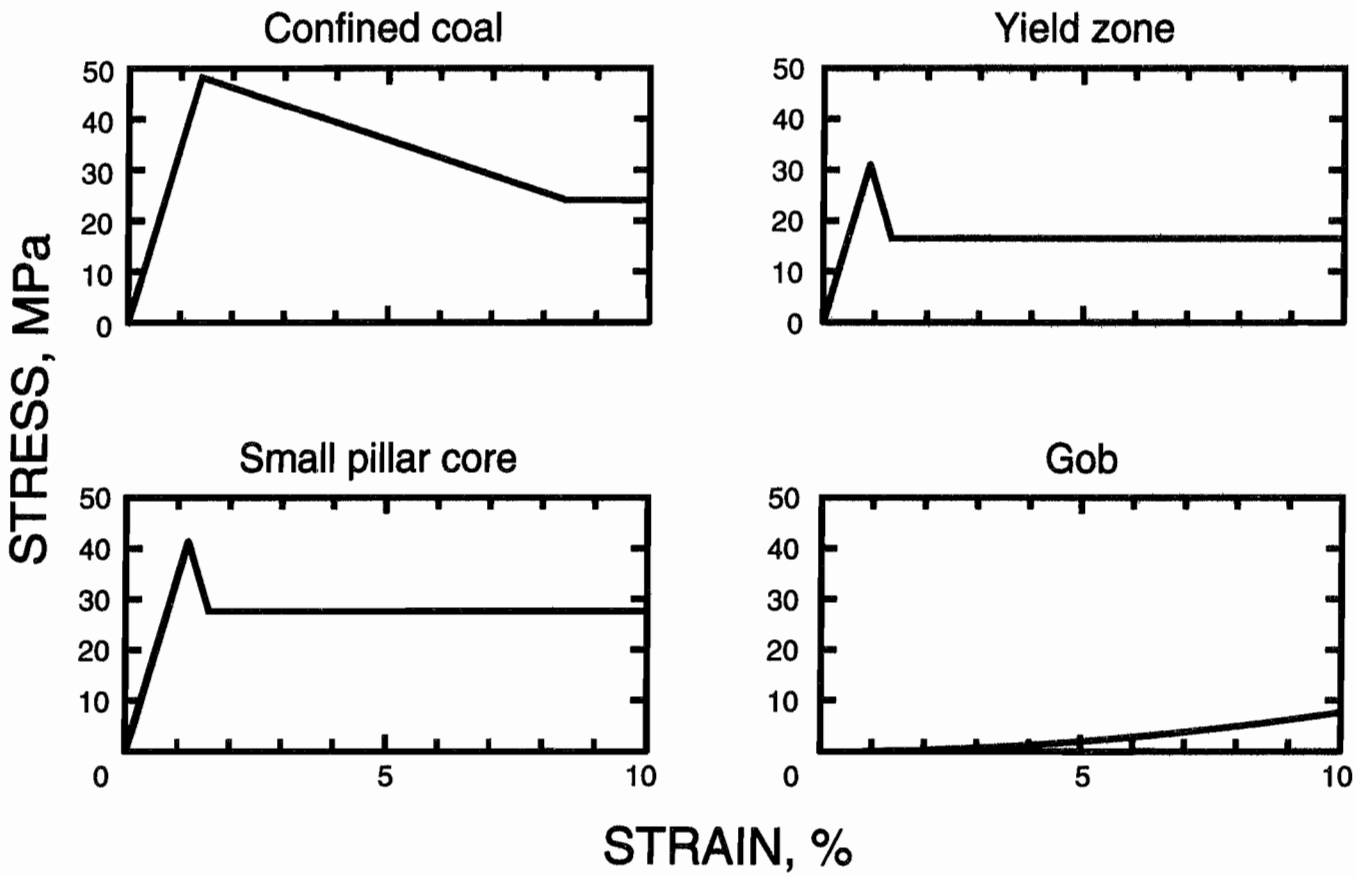

Figure 7.—Coal-element properties, Model B analyses.

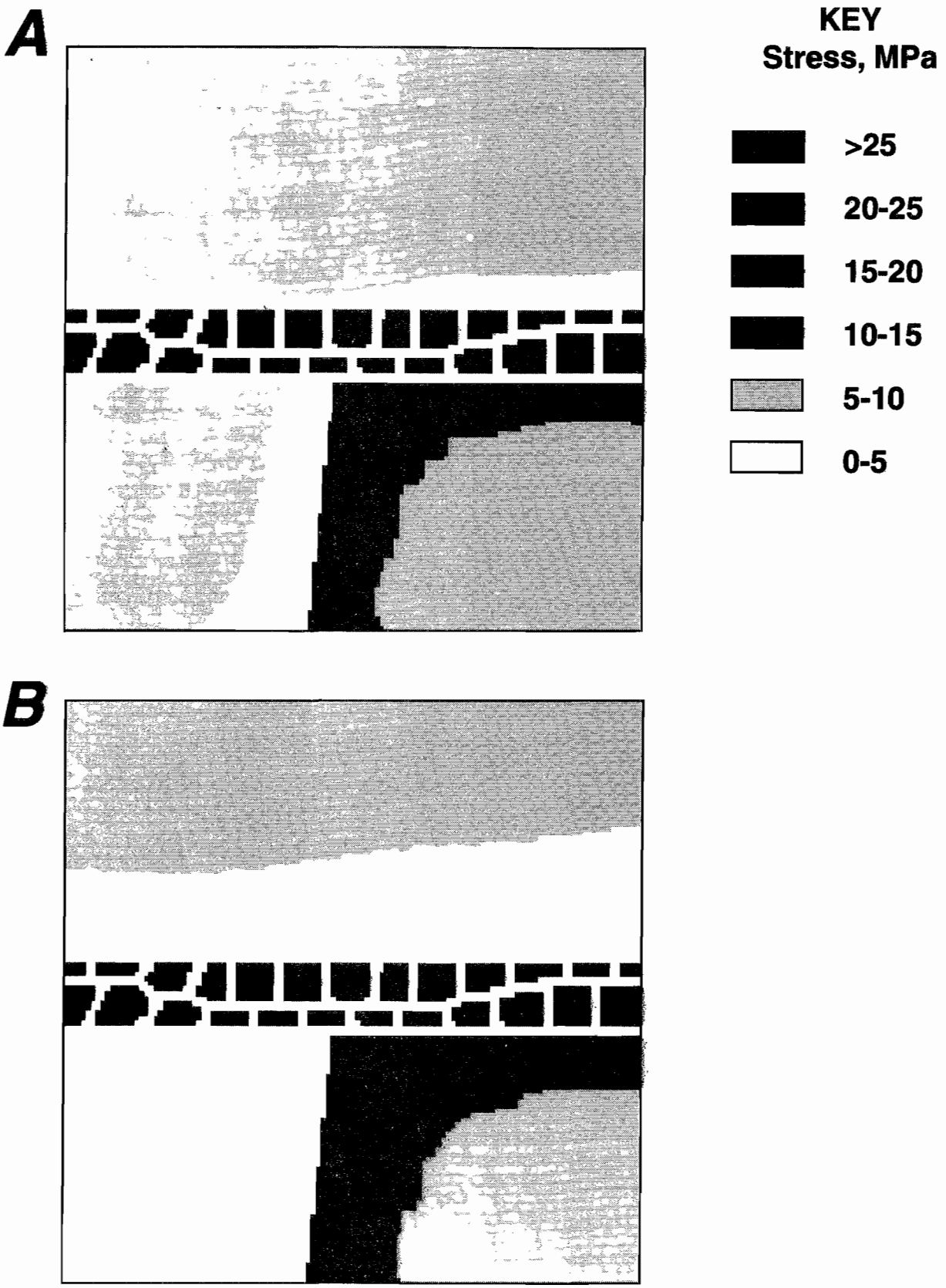

Figure 8.—Model A and B analyses of alternative gate road test site.

FIELD MONITORING

Prior to the mining of panel 4, directional BPCs were installed in the alternative gate road test site to monitor vertical ground pressure changes within the coal structures during the extraction of panels 4 and 5. The position and locations of these BPCs are shown in figure 3. During the mining of panel 4, the gate road test site was monitored as a headgate structure. Later, during the mining of panel 5, the gate road test site was monitored as a tailgate structure.

GROUND PRESSURE INSTRUMENTATION

Directional BPCs were developed by USBM researchers during the late 1950's and have been used extensively to monitor ground pressure changes in coal mines. Equipment designs and installation procedures are described in detail by others, and several techniques for converting BPC pressure data to ground stress measurements have been proposed in the technical literature (*6*). Basically, the cells consist of small hydraulic flat jacks encapsulated in cement for insertion in NX-size boreholes. After the cell is positioned in the drill hole, it is typically preloaded to a value approximately equal to the assumed overburden stress (about 8.3 MPa (1,200 psi) in this study).

After the BPCs were installed at the test site, they were fitted with pressure transducers and connected to the USBM computer-assisted GCMS. Subsequently, the field data monitored by the GCMS are transferred to the USBM central control computer at the Denver Federal Center where they can be continuously monitored, stored, and analyzed by USBM researchers.

The BPCs are designated by a code that describes the mine location, drill hole position, and depth of placement into the coal structure. For example, 1YPI-22 references a BPC installed from entry No. 1 into the small pillar to a depth of 7 m (22 ft). Similarly, 2BPI-45 references a cell installed from entry No. 2 into the large pillar to a depth of 14 m (45 ft).

The BPCs located in the test section were continuously monitored, using the GCMS, throughout their useful lives during the mining of panels 4 and 5.

GROUND PRESSURE DATA ANALYSIS TECHNIQUES

Several techniques for converting BPC pressure data to coal stress measurements have been proposed in the technical literature (*6*). To provide a basis for comparison between the BPC and MULSIM/NL data used in this study, a simple rationale for converting BPC pressure to vertical ground stress was needed. Observing that the pressure cells were installed at various gate road sites to measure changes and trends in the distribution of vertical loads on the coal structures in response to longwall mining, a simplifying assumption based on a review of earlier published data was made. The vertical stress within the coal mine structures was assumed to be 80% of the BPC pressure change monitored after installation of the BPC plus the addition of a preexisting vertical stress of 8.3 MPa (1,200 psi) created by the overburden load.

This technique was used to analyze the BPC data from previous instrument sites, and to develop the nonlinear coal strength properties used in the MULSIM/NL Model B analyses (see previous section on Selection of Coal-Element Properties). This simplified rationale was also used to analyze and reduce the BPC data from the new alternative gate road test site for comparison with the MULSIM/NL model analyses.

EVALUATION OF GATE ROAD PERFORMANCE

Field observations of improved tailgate roadway conditions in the new alternative gate road field test site area agree well with the qualitative predictions of the MULSIM/NL models. Mine roof conditions in the tailgate roadway immediately outby the face were generally good in the test site area, compared to the typical development of cutter-type roof failures in the tailgate roadway of the existing gate road system. Also, the development of floor heave and associated deterioration of the ribs were less pronounced. These observations all indicate that the tailgate roadway of the alternative gate road system is exposed to reduced abutment stress levels, thus resulting in improved ground conditions. A detailed analysis of the BPC data versus the MULSIM/NL model predictions also supports these observations.

PANEL ABUTMENT PRESSURES

Four BPCs were installed parallel to the longwall face in panel 5 at depths of 3, 6, 9, and 12 m (10, 20, 30, and 40 ft) within a borehole drilled from the tailgate roadway (entry No. 1) of panel 5 as shown in figure 3. These BPCs were installed to monitor the ground pressure abutment changes ahead of the face as panel 5 was mined. They

were also monitored during the mining of panel 4 to detect any changes resulting from the development of a side abutment that might be created by the mining of panel 4. The resulting pressure data were converted to vertical stress changes using the rationale previously explained in the section on Ground Pressure Data Analysis.

During the mining of panel 4, only cells 1P5I-10 and 1P5I-20 were monitored, and the resulting data are shown in figure 9*A*. These pressure cells began to detect pressure changes when the face of panel 4 was about 60 m (200 ft) inby the instrument site, and indicated a steady increase until the cells were disconnected from the GCMS when the face was about 240 m (800 ft) outby the instrument site. The total pressure increase was about 5 MPa (750 psi) for cell 1P5I-10, located 3 m (10 ft) into the tailgate rib of panel 5, and 3.5 MPa (500 psi) for cell 1P5I-20, located 6 m (20 ft) into the panel. These increases are in general agreement with the ground pressure changes to be expected from the development of a side abutment pressure zone created by the mining of panel 4. The field monitored pressure changes also agree well with those predicted by the MULSIM/NL Model A and B analyses, as shown in figures 9*B* and 9*C*, respectively. Model B analyses predicted pressure changes in the range of 2 to 3 MPa (300 to 400 psi), whereas Model A analyses predicted changes in the range of 1.5 to 2 MPa (200 to 300 psi).

All four of the BPCs installed in panel 5 were connected to the GCMS to monitor ground pressure changes during the mining of panel 5. The resulting data are plotted in figure 10*A*, and show the general development of the ground pressure abutment ahead of panel 5. The BPCs indicate that for practical purposes the ground pressure responses are elastic in nature relative to the location of the longwall face, with little indications of time-dependent loading. The maximum ground pressure changes prior to the mine-through of the instruments are in the range of 41 to 48 MPa (6,000 to 7,000 psi), with all of the instruments recording a similar loading pattern. Pressure cell 1P5I-10 did yield at a load of 38 MPa (5,500 psi) when the face was about 20 m (65 ft) inby the cell; however, this behavior is interpreted to be an indication of rib yielding and sloughage because of its close proximity (3 m (10 ft)) to the tailgate roadway as the face advanced upon the instrument site. Field observations indicated rib sloughage developing about 25 m (80 ft) ahead of the longwall face. The BPC data also indicate that the width of the pressure abutment ahead of the longwall face is about 45 m (150 ft).

The pattern of field monitored ground pressure changes ahead of the longwall panel agrees in general with those predicted by the MULSIM/NL models (see figures 10*B* and 10*C*). The width of the abutment zone is predicted by both model analyses to be in the range of 35 to 45 m (100 to 150 ft) ahead of the longwall face. The Model A analysis predicts a peak abutment pressure change of 24 MPa (3,500 psi), whereas the Model B analysis predicts a peak pressure change of 33 MPa (4,800 psi). In general, it is concluded that the MULSIM/NL model analyses can be reliable predictors of the relative magnitude and extent of the pressure abutment ahead of a longwall face.

SMALL-PILLAR BEHAVIOR

Three BPCs were installed in the small pillar parallel to the longwall faces of panels 4 and 5 at depths of 2.4, 4.5, and 7 m (8, 15, and 22 ft) within a borehole drilled from the tailgate roadway (entry No. 1) of panel 5 as shown in figure 3. These BPCs were installed to monitor the behavior of the small pillar as both panels 4 and 5 were mined. The resulting pressure data were converted to vertical stress changes using the rationale previously explained in the section on Ground Pressure Data Analysis. During the mining of panels 4 and 5, all three cells (1YPI-8, 1YPI-15, and 1YPI-22) were monitored by the GCMS, and the resulting data are shown in figures 11*A* and 12*A*.

The pressure cells began to detect pressure changes when the face of panel 4 was about 60 m (200 ft) inby the small-pillar instrument site, and indicated a steady pressure increase until the cells were disconnected from the GCMS when the face was about 240 m (800 ft) outby the instrument site. The total pressure increases monitored during the mining of panel 4 ranged from about 9.7 MPa (1,400 psi) for cell 1YPI-8, located 2.4 m (8 ft) into the rib from the tailgate roadway (entry No. 1) of panel 5, to 13.1 MPa (1,900 psi) for cell 1YPI-22, located 2.4 m (8 ft) from the rib line of entry No. 2 (nearest to panel 4). Cell 1YPI-15 was located in the center of the small pillar and monitored a pressure change of 11 MPa (1,600 psi). These pressure increases are in general agreement with the ground pressure changes to be expected from the development of a side abutment pressure zone created by the mining of panel 4. The general pattern and sequence of field monitored pressure changes agrees well with the predictions of the MULSIM/NL Model A and B analyses, as shown in figures 11*B* and 11*C*; however, the models predicted pressure changes in the range of 3 to 6 MPa (400 to 800 psi), which is much less than the magnitude of those monitored by the pressure cells.

During the mining of panel 5, the BPC data indicate that the ribs of the small pillars began to yield and slough about 400 ft outby the longwall face as shown in figure 12*A*. The load on the central portion of the small pillar increased to about 48 MPa (7,000 psi) before the

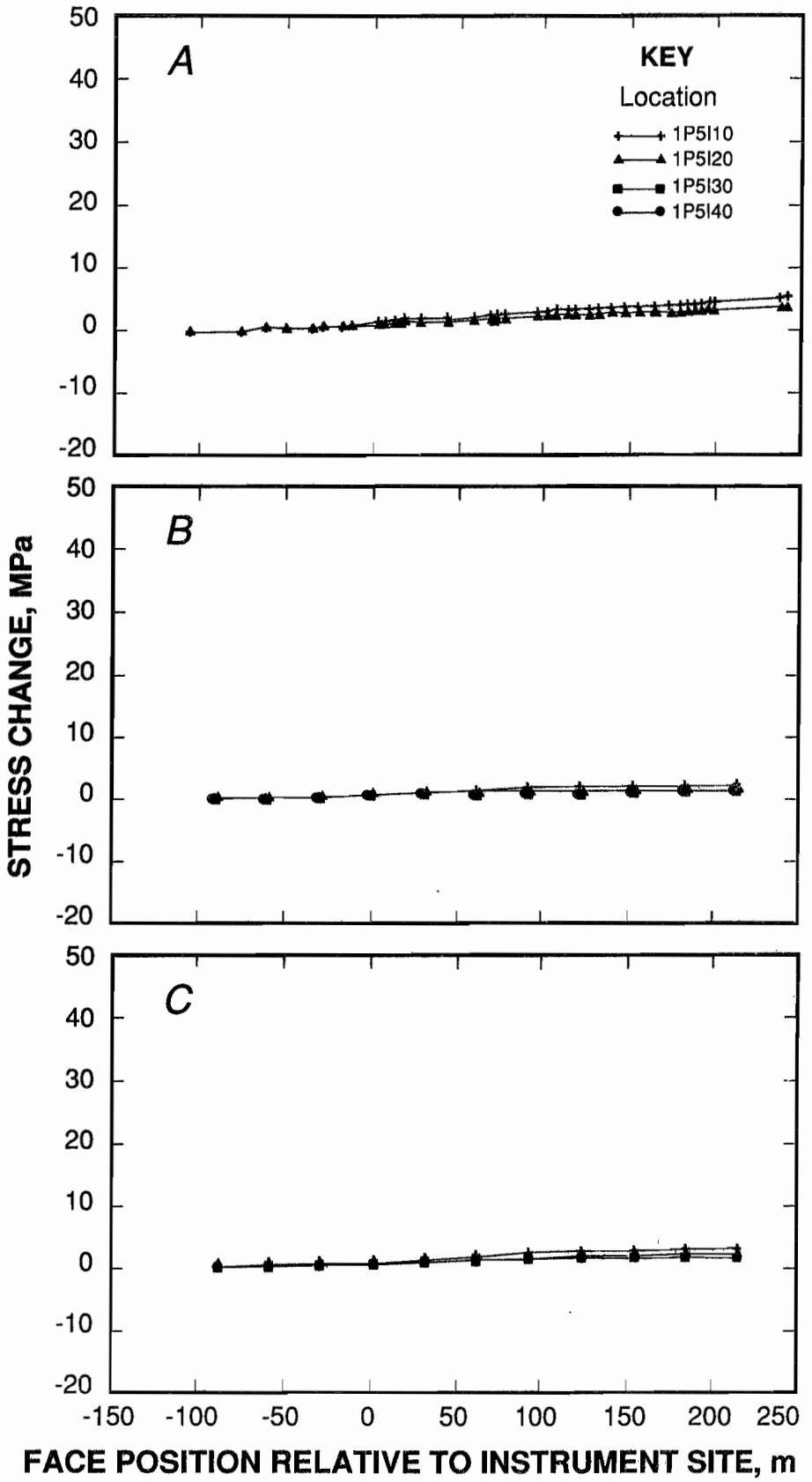

Figure 9.—Comparison plots of Panel Abutment BPC data and MULSIM/NL model stress projections during the mining of Panel 4.

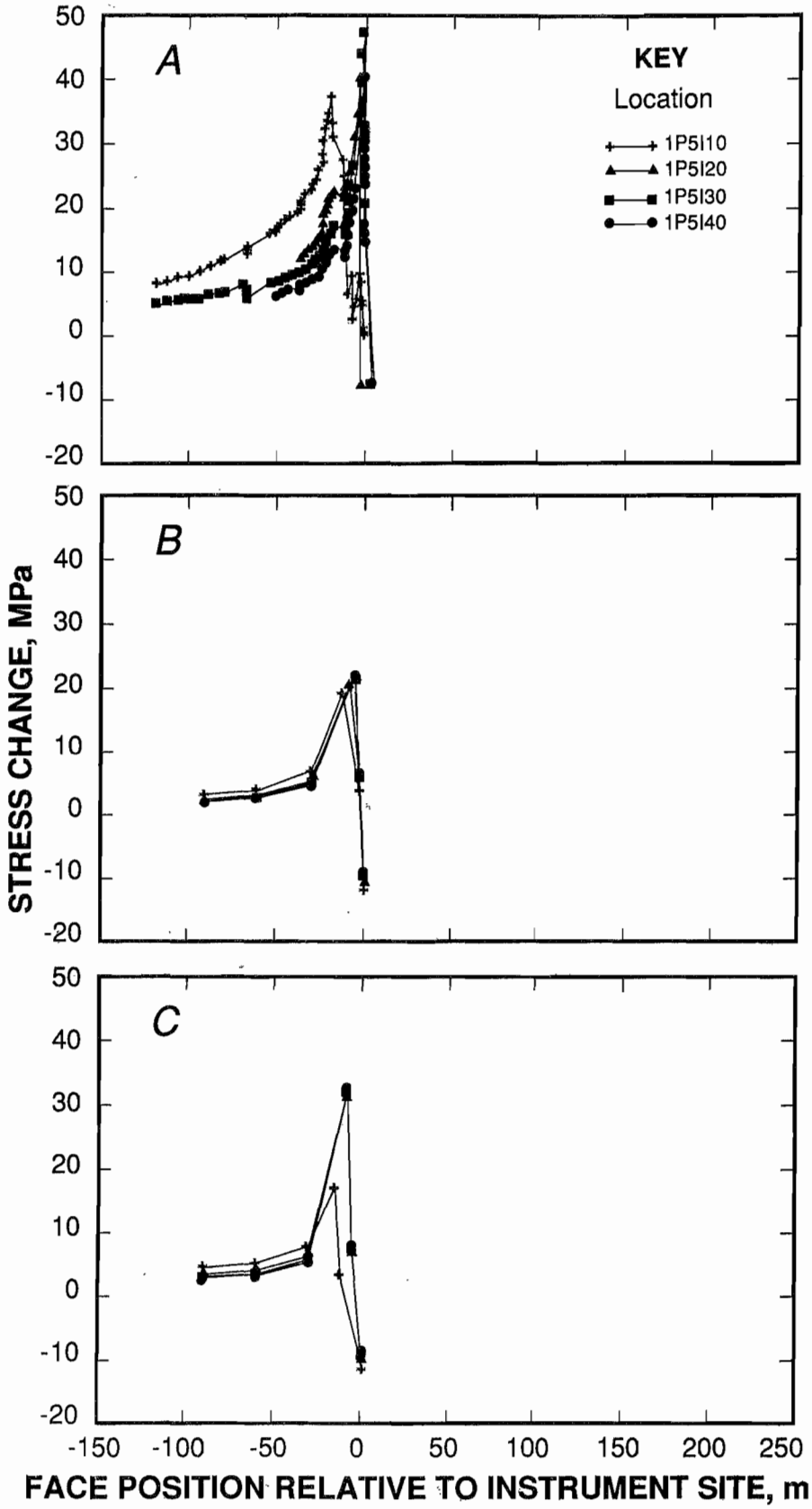

Figure 10.—Comparison plots of Panel Abutment BPC data and MULSIM/NL model stress projections during the mining of Panel 5.

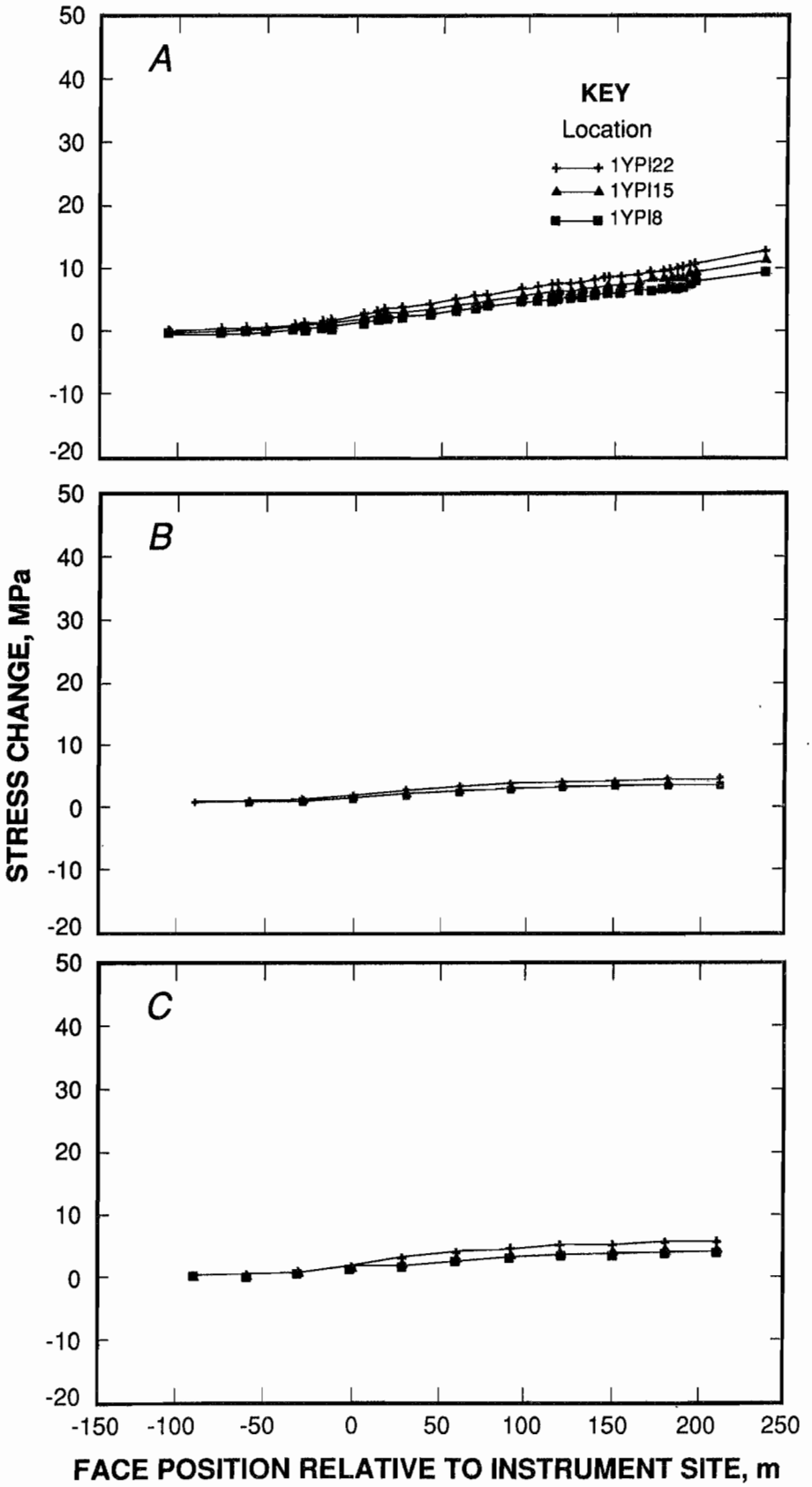

Figure 11.—Comparison plots of small-pillar BPC data and MULSIM/NL model stress projections during the mining of Panel 4.

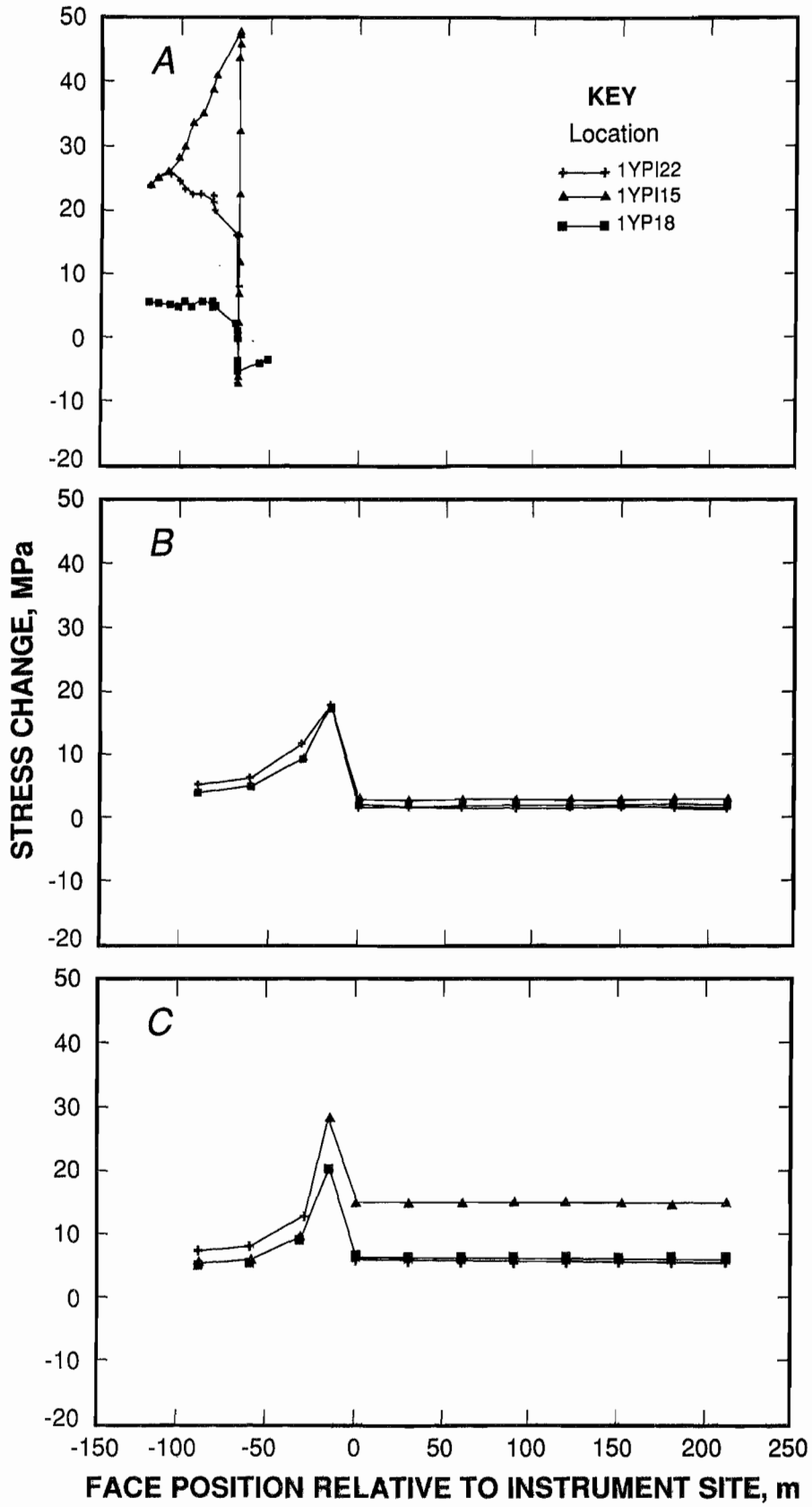

Figure 12.—Comparison plots of small-pillar BPC data and MULSIM/NL model stress projections during the mining of Panel 5.

pillar completely failed about 60 m (200 ft) outby the longwall face. The MULSIM/NL Model A and B analyses predicted that the small pillar would begin to take load about 60 m (200 ft) outby the face and begin to fail about 20 m (65 ft) outby the face as shown in figures 12*B* and 12*C*, respectively. Again the general pattern and sequence of loading predicted by the model analyses are in agreement with the field measurements and observations. The peak pressure changes on the ribs of the small pillar predicted by the models are in the range of 20 MPa (3,000 psi) and agree reasonably well with the field monitored pressure changes ranging from 7 to 24 MPa (1,000 to 3,500 psi). Models A and B predict the pressure increase at failure within the core of the small pillar to be about 21 MPa (3,000 psi) and 28 MPa (4,100 psi), respectively, as compared to the field measurement of 48 MPa (7,000 psi).

The MULSIM/NL models can account for the residual strength in the failed coal pillars; but by their design, the BPCs are not very effective tools for measuring the residual strength of failed coal pillars. In general, it is concluded that the MULSIM/NL model analyses can be used to predict the relative loading and failure sequence of the small gate road pillars.

LARGE-PILLAR BEHAVIOR

Five BPCs were installed in the large pillar parallel to the longwall faces of panels 4 and 5 at depths of 3, 6, 13.7, 21, and 24 m (10, 20, 45, 70, and 80 ft) within a borehole drilled from the central roadway of the gate road system (entry No. 2) as shown in figure 3. These BPCs were installed to monitor the behavior of the large pillar as both panels 4 and 5 were mined. The resulting pressure data were converted to vertical stress changes using the rationale previously explained in the section on Ground Pressure Data Analysis.

During the mining of panel 4, all five ground pressure cells (2BPI-10, 2BPI-20, 2BPI-45, 2BPI-70, and 2BPI-80) were monitored by the GCMS, and the resulting data are shown in figure 13*A*. Because cell 2BPI-80 failed during the mining of panel 4, only the four remaining cells were monitored during the mining of panel 5, and the resulting data are shown in figure 14*A*.

The pressure cells began to detect pressure changes when the face of panel 4 was about 60 m (200 ft) inby the large pillar instrument site, and indicated major pressure changes when the face was about 15 m (50 ft) inby the instrument site. The magnitude of pressure changes within the gate road system decreased with distance from the edge of panel 4. The monitored ground pressures steadily increased as panel 4 mined outby the instrument site until the pressure cell (2BPI-80) nearest to the edge of panel 4 peaked at a stress change of 17 MPa (2,500 psi) and began to decrease when the face of panel 4 was about 180 m (600 ft) outby the site (see figure 13*A*). This pressure decrease is interpreted as rib failure and sloughage of the large pillar adjacent to the gob of panel 4.

When panel 5 was about 80 m (270 ft) inby the instrument site (see figure 14*A*), cell 2BPI-10, located 3 m (10 ft) into the rib of the large pillar from entry No. 2, also peaked at a pressure change of 21 MPa (3,000 psi) and failed, indicative of failure and sloughage of the rib of the pillar. When panel 5 was about 40 m (130 ft) inby the instrument site, the load on both pressure cells 2BPI-20 and 2BPI-70 (located 6 m (20 ft) inside the rib lines on either side of the large pillar) peaked and the pillar began to fail, shifting increased load onto the center of the pillar. The peak pressure changes were in the range of 34 MPa (5,000 psi) and 48 MPa (7,000 psi), respectively, for cells 2BPI-20 and 2BPI-70. The cells both indicated complete pillar failure as panel 5 mined past the instrument site. The pressure cell located in the center of the pillar (2BPI-45) reached a peak pressure change of 48 MPa (7,000 psi) when the face of panel 5 was about 30 m (100 ft) inby the site. This peak pressure was maintained until the face mined past the site and the instrument connections were lost. These ground pressure changes and failures are in general agreement with what is to be expected from the interactions of the side abutment pressure zone created by the mining of panel 4 and the frontal abutment pressure created by the mining of panel 5.

The general pattern and sequence of field monitored pressure changes and failures within the large pillar agrees with the predictions of the MULSIM/NL model analyses. Model A analyses are shown in figures 13*B* and 14*B*, and Model B analyses are shown in figures 13*C* and 14*C*. For example, Model A predicted that pressure cell 2BPI-80, located 3 m (10 ft) from the gob of panel 4, would peak at a stress change of 18 MPa (2,600 psi) as compared with the field measurements of 21 MPa (3,000 psi). Failure was predicted to occur when the face of panel 4 was about 90 m (300 ft) outby the instrument site as compared to field indications that increased loading occurred when the face of panel 4 was about 180 m (600 ft) outby the site. Model B had predicted a peak load of 15 MPa (2,200 psi) about 30 m (100 ft) outby the site. In addition Model A predicted the progressive loading and sequential failure of the large pillar as monitored in the field as the face of panel 5 approached the instrument site.

SUMMARY EVALUATION

To facilitate a realistic comparison of the MULSIM/NL model predictions and field measurements made at the mine test site, several stress profiles have been constructed as shown in figures 15 and 16. These stress profiles show the progressive changes in load conditions predicted by

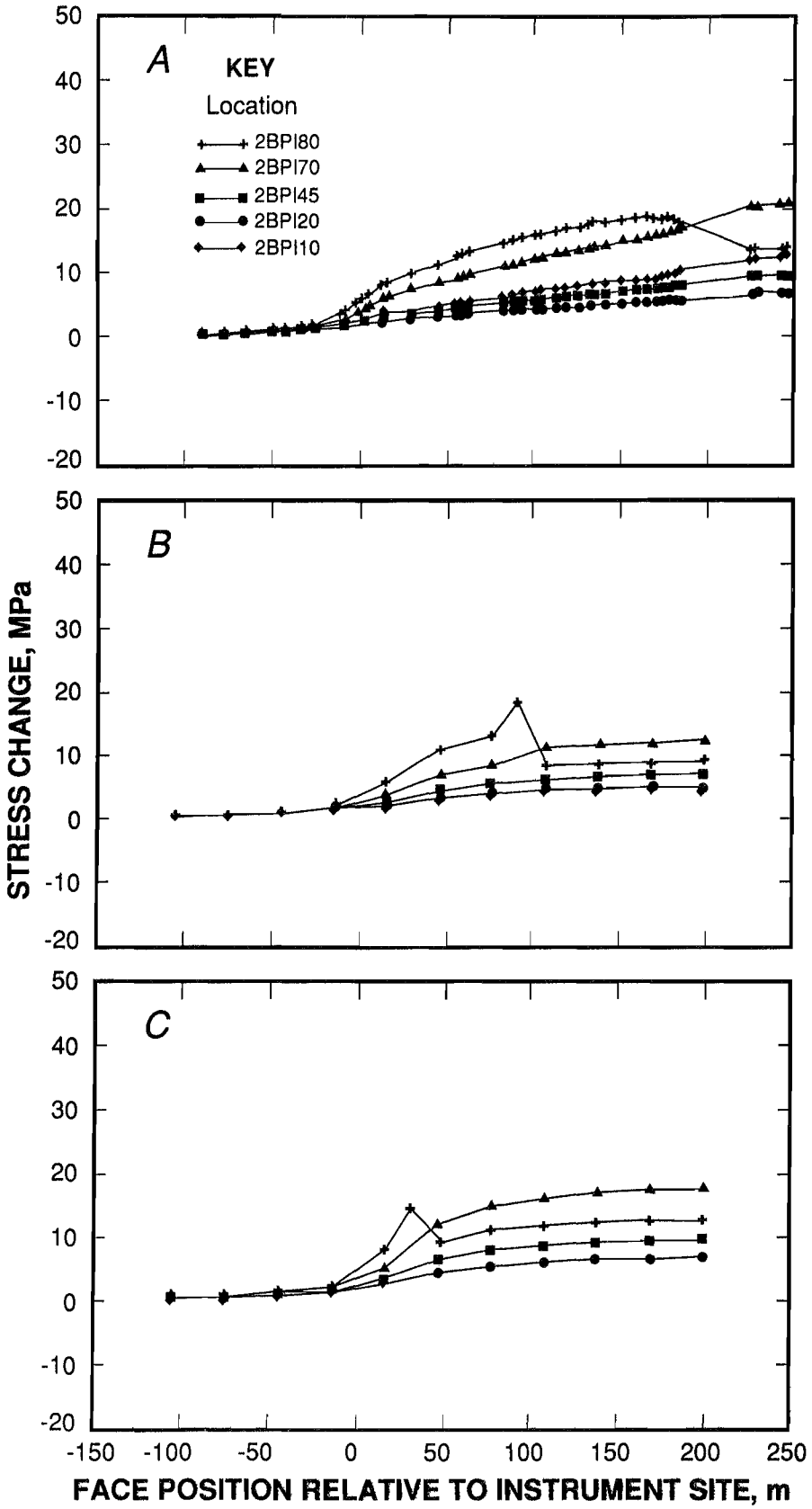

Figure 13.—Comparison plots of large-pillar BPC data and MULSIM/NL model stress projections during the mining of Panel 4.

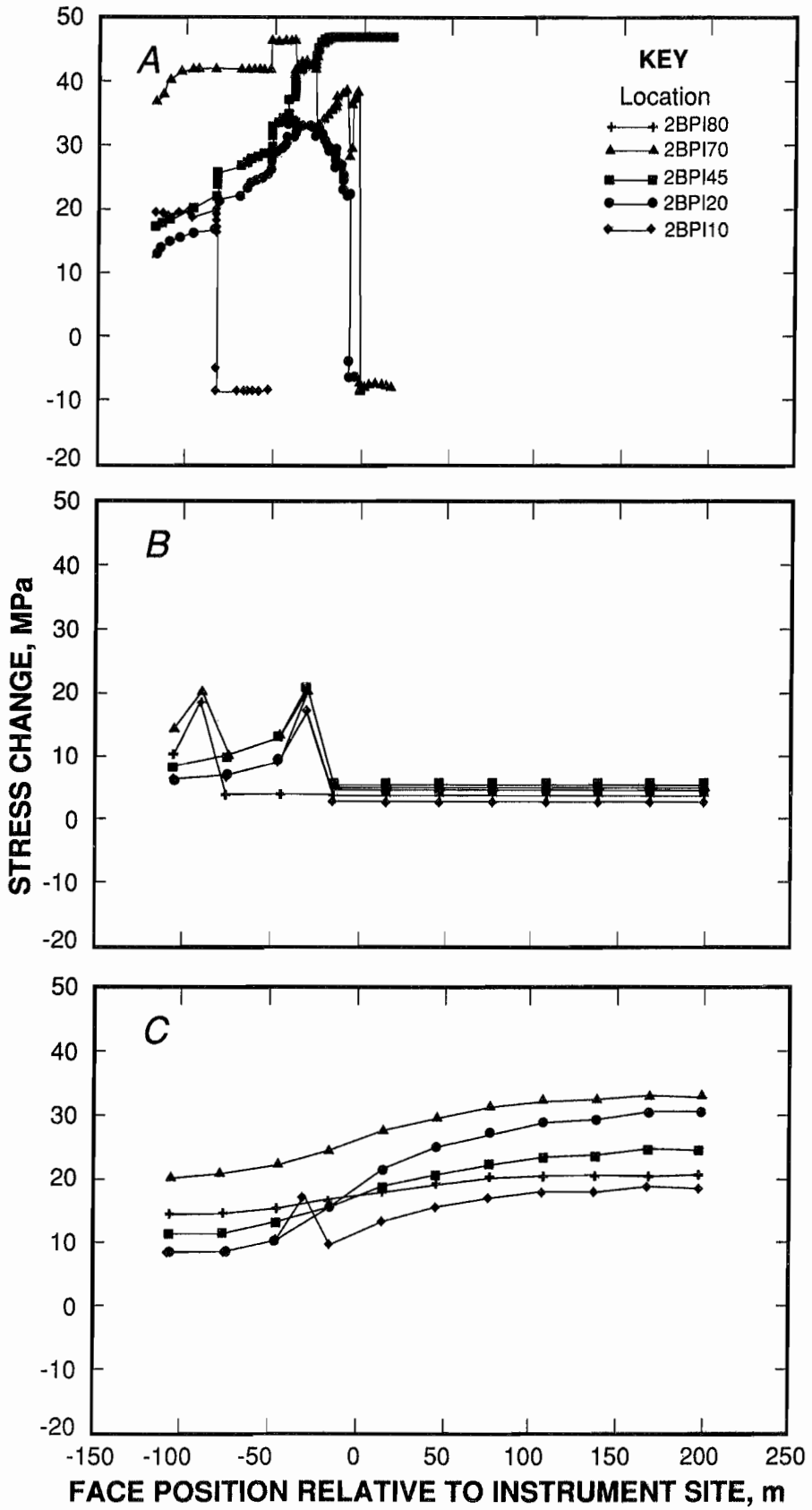

Figure 14.—Comparison plots of large-pillar BPC data and MULSIM/NL model stress projections during the mining of Panel 5.

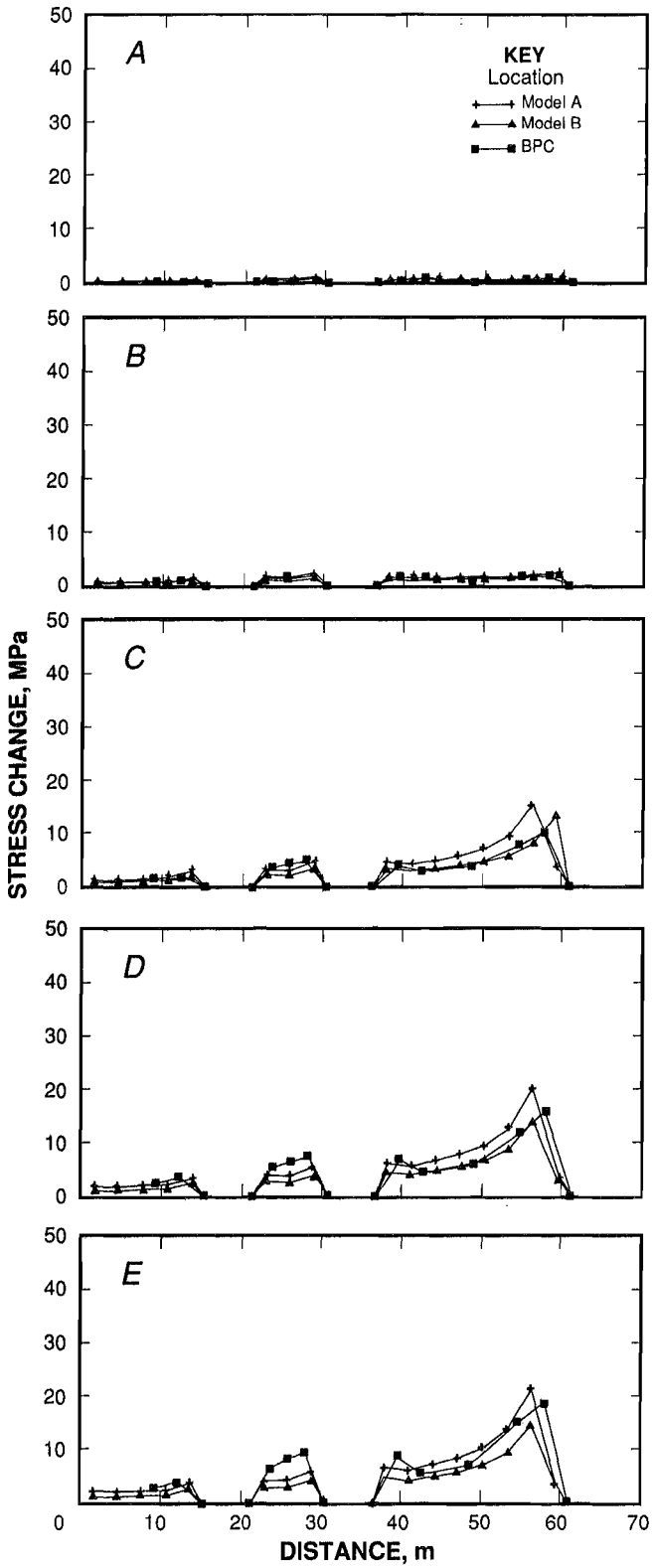

Figure 15.—Plots of MULSIM/NL and BPC data comparisons during the mining of Panel 4.

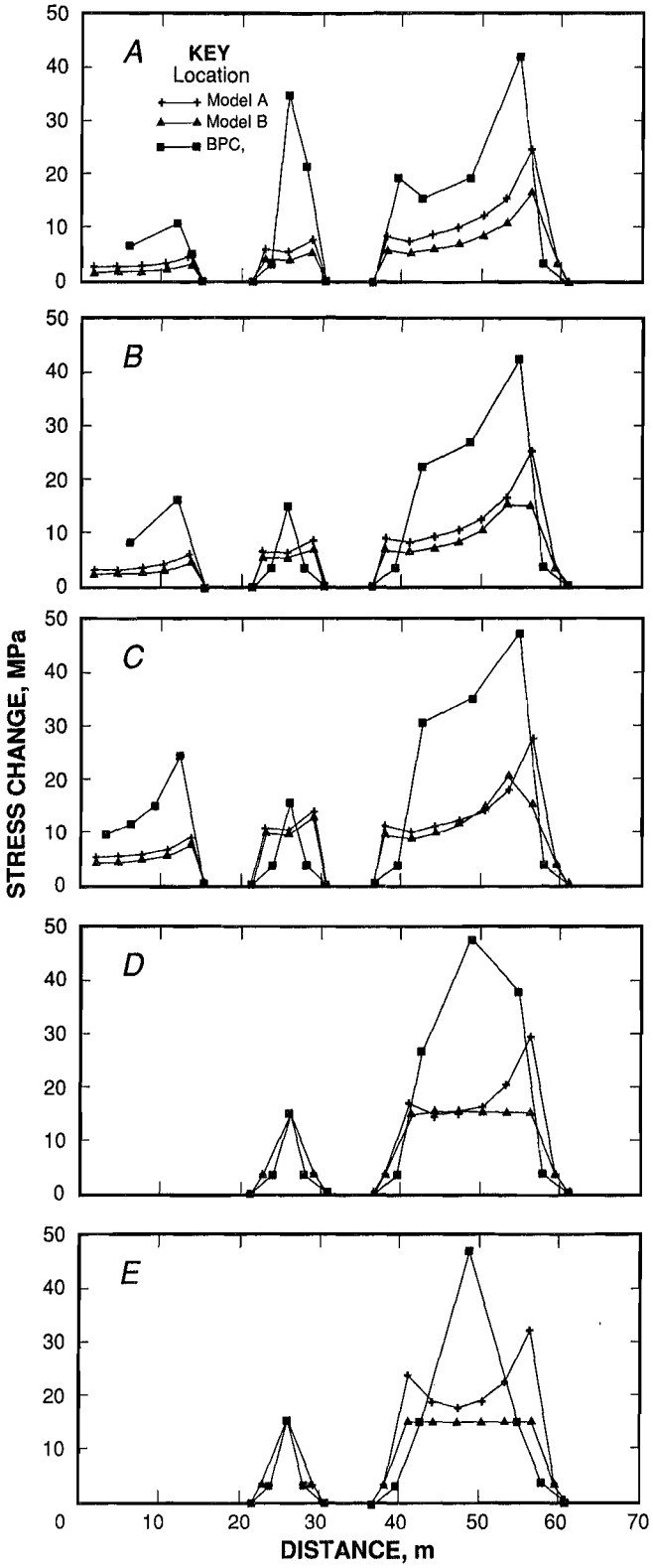

Figure 16.—Plots of MULSIM/NL and BPC data comparisons during the mining of Panel 5.

Models A and B, and measured by BPCs at critical stages during the mining of both panels 4 and 5 adjacent to the field test site.

Figures 15*A* through 15*E* show the progressive development of the side abutment pressure zone as panel 4 is mined past the test site. The MULSIM/NL model predictions and the field measured ground pressures are in good agreement. The data indicate that the gob side rib of the larger pillar yields and fails as panel 4 is mined by the test site, and that the abutment profile develops as predicted by the models. Field observations support the conclusion that the alternative gate road pillar pattern shifts the higher abutment loads toward the gob and thus provides better protection to the tailgate roadway of the next panel to be mined.

Figures 16*A* through 16*E* show the progressive interactions of the frontal abutment pressure zone ahead of panel 5 and the side pressure abutment zone from panel 4 on the loading of the gate road pillar system. The data indicate that the small pillar ribs begin to load up progressively and slough when the face of panel 5 is within 92 m (300 ft inby) of the test site, and that for practical purposes the small pillar has yielded as the face mines past the pillar. Likewise the panel 5 side of the large pillar progressively loads and yields as the face of panel 5 mines through the area, and only the central core of the large pillar is carrying high pressure after panel 5 is mined.

The Model A and Model B analyses are in general agreement with field observations and measurements made during mining. Of the two, Model A is in closer agreement with regards to yielding of the large pillars. Both models significantly underestimated peak pressure changes in the coal structure as determined by field measurements; in the case of the peak frontal abutment pressure, field values are three times those predicted by the models. A possible explanation is that the pressure loading characteristics of the BPCs are nonlinear and affected by the bilateral stress field present in the abutment zone. Even so, both model analyses predict the general sequence of loading and yielding of the gate road pillar system. Thus it is concluded that the value of the MULSIM/NL techniques as a reliable design tool has been verified by this field experiment.

The field experiment also has validated the proposed alternative gate road system, under existing conditions, for providing protection to the tailgate roadway escape route necessary for the successful operation of the high-speed mechanized longwall mining systems being used at the mine.

CONCLUSIONS

The field test has confirmed the validity of the new alternative gate road system under actual mining conditions. Field observations indicated that the alternative gate road design significantly improved tailgate roadway stability under existing ground conditions.

Field measurements support the results of the model analyses that suggested that reversing the gate road pillar arrangement would shift the higher abutment loads toward the gob of the previous panel and away from the tailgate of the current panel, thus reducing ground pressures and improving tailgate ground conditions.

The study has shown that the MULSIM/NL modeling technique can be used with confidence as a coal mine design tool. The field measurements confirm that the MULSIM/NL models predict the general pattern and magnitude of ground stresses expected to develop in and around a longwall panel. The model analyses also remarkably predicted the pattern and sequence of abutment loading and the progressive yielding and failure of coal ribs and pillars.

The study also shows that the critical factor in applying the MULSIM/NL modeling technique is a careful evaluation of geomechanical data and the selection of appropriate material properties for the model elements. The MULSIM/NL technique provides the mine design engineer with a powerful design tool for site-specific applications, that can be used with confidence to improve ground control conditions under actual mining conditions.

REFERENCES

1. Zipf, R. K. MULSIM/NL Application and Practitioner's Manual. USBM IC 9322, 1992, 48 pp.

2. Hanna, K., and R. Cox. Automated Ground Control Management System for Coal Mine Hazard Detection. Paper in Proceedings of 2nd International Symposium on Mine Mechanization and Automation (Lulea, Sweden, June 7-10, 1993). Balkema, 1993, pp. 681-689.

3. Conover, D., K. Hanna, and T. Muldoon. Mine-Wide Monitoring Applications in Ground Control Research. Paper in Proceedings of 9th Conference on Ground Control in Mining, WV Univ., Morgantown, WV, June 1990, pp. 135-141.

4. Hanna, K., K. Haramy, and T. R. Ritzel. Automated Longwall Mining for Improved Health and Safety at the Foidel Creek Mine. Soc. Min. Eng. AIME, preprint 91-165, 1991, 11 pp.

5. Peng, S. S., and H. S. Chiang. Longwall Mining. Wiley, 1984, 708 pp.

6. Haramy, K., and R. O. Kneisley. Hydraulic Borehole Pressure Cells: Equipment, Techniques, and Theories. USBM IC 9294, 1991, 26 pp.

APPENDIX A.—TYPICAL MULSIM/NL MODEL FORMULATION

Appendix A contains a printout of a typical computer input used in this study to demonstrate the steps involved in the formulation of a MULSIM/NL model.

```
BOBTOM6.INP  EXISTING GATEROAD ANALYSIS, 120 x120 elements
0.2500000.120000E+07       1
       6
    2.00.450E+04.110E-01.225E+04.165E-01.250E+00
    3.00.500E+04.120E-01.000E+00.250E+00.000E+00
    3.00.300E+04.750E-02.000E+00.250E+00.000E+00
    2.00.450E+04.110E-01.225E+04.165E-01.250E+00
    3.00.100E+04.250E-02.000E+00.250E+00.000E+00
    6.00.400E+05.160E+05.300E+01.000E+00.000E+00
    0.0.0917    0.0.0000    0.0.0000    0.0.0917    0.0.0000    0.0.0917
  600.00       50       50                          14       37       14       37
     0.0      0.0-13200.0   120.0
 1.00000 0.00000 0.00000 0.00000 1.00000 0.00000 0.00000 0.00000 1.00000
    1.35   25.00      100                                  1        1
```

Figure A-1.—Input parameters used for initial MULSIM/NL model formulations.

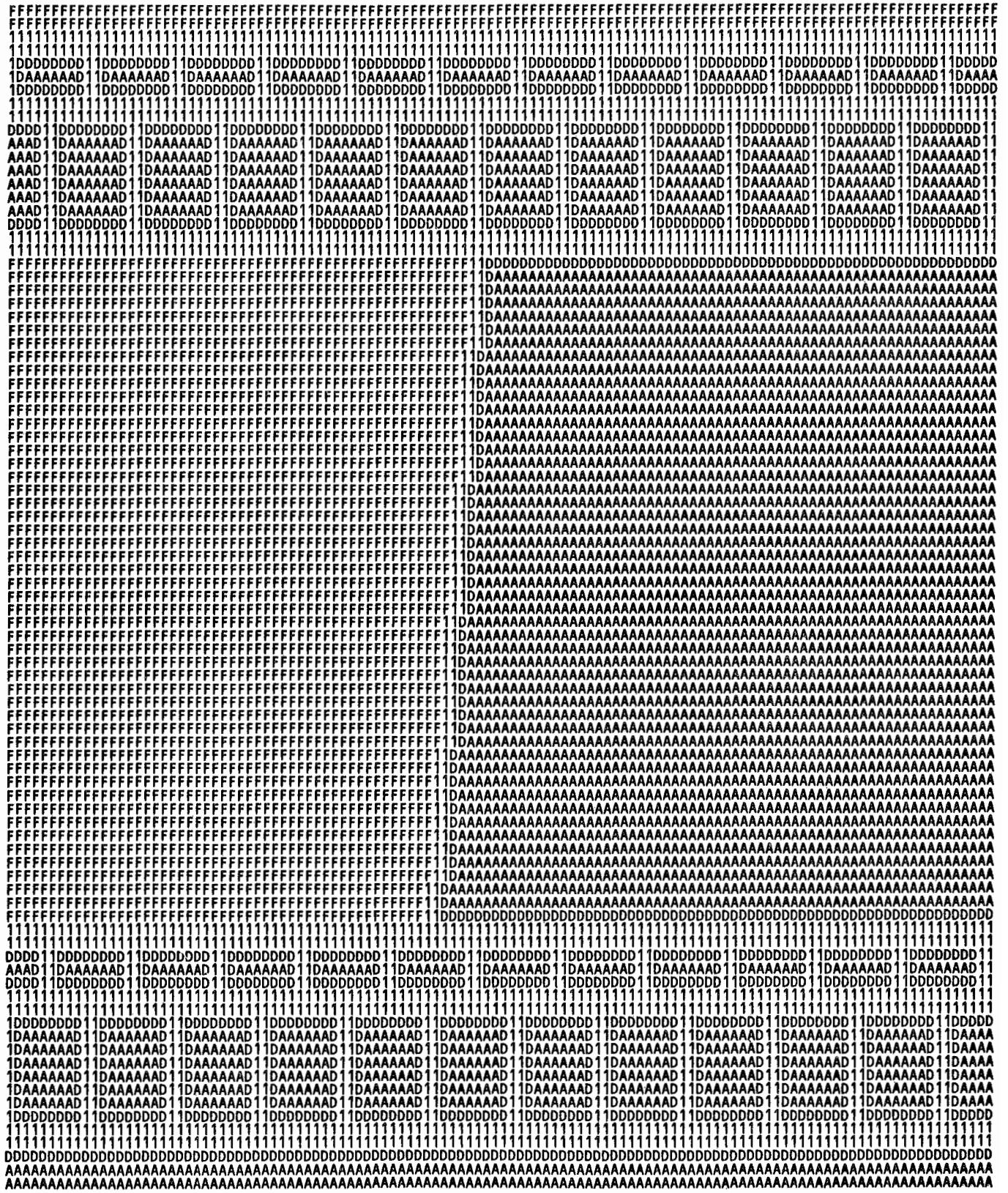

Figure A-2.—Partial fine mesh of existing gate road layout.

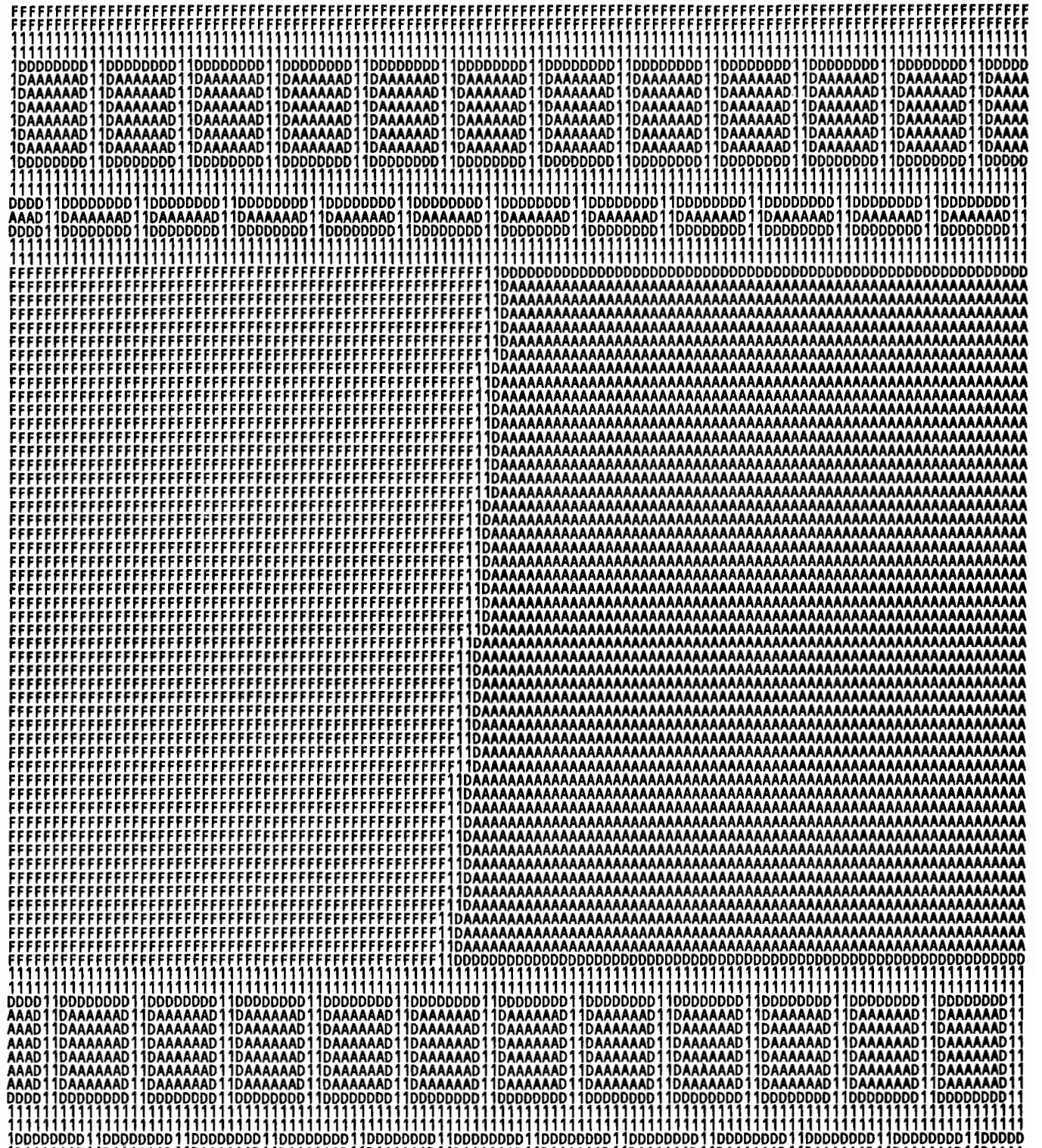

Figure A-3.—Partial fine mesh of proposed alternative gate road layout.

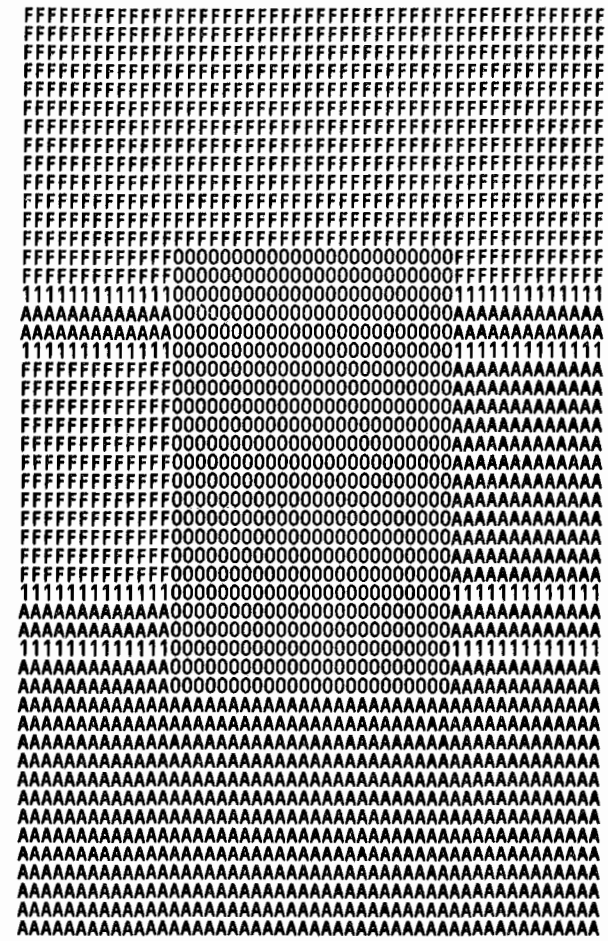

Figure A-4.—Coarse mesh for initial MULSIM/NL model analyses.

APPENDIX B.—ALTERNATIVE GATE ROAD MULSIM/NL MODELS

The details of the input data for each of the alternative gate road test site MULSIM/NL models are presented in appendix B.

```
FLIB1002.INP    EXPERIMENTAL GATEROAD ANALYSIS - MODEL A, NON-LINEAR, 120 x 120 elements
0.2500000.100000E+07       1
      14
    1.00.500E+06.200E+06.000E+00.000E+00.000E+00
    3.00.750E+04.150E-01.125E+06.250E+00.000E+00
    2.00.450E+04.113E-01.225E+04.165E-01.250E+00
    3.00.200E+04.400E-02.000E+00.250E+00.000E+00
    2.00.450E+04.113E-01.225E+04.165E-01.250E+00
    6.00.400E+05.160E+05.300E+01.000E+00.000E+00
    6.00.100E+06.400E+05.300E+01.000E+00.000E+00
    6.00.300E+06.120E+06.300E+01.000E+00.000E+00
    6.00.200E+07.800E+06.300E+01.000E+00.000E+00
    6.00.400E+05.160E+05.300E+01.000E+00.000E+00
    3.00.300E+04.300E-01.250E+05.250E+00.000E+00
    3.00.300E+04.100E-01.750E+05.250E+00.000E+00
    3.00.300E+04.150E-02.500E+06.250E+00.000E+00
    2.00.450E+04.113E-01.225E+04.165E-01.250E+00
    0.0.0917    0.0.0000    0.0.0000    0.0.0917    0.0.0000    0.0.0917
  600.00      50      50                          14      37      14      37
     0.0     0.0-13200.0   120.0
 1.00000 0.00000 0.00000 0.00000 1.00000 0.00000 0.00000 0.00000 1.00000
    1.35  100.00     200                                   1       1
```

Figure B-1.—Input parameters for test site Model A.

```
TLIB1002.INP    EXPERIMENTAL GATEROAD ANALYSIS - MODEL B, NON-LINEAR, 120 x 120 elements
0.2500000.100000E+07       1
      14
    1.00.500E+06.200E+06.000E+00.000E+00.000E+00
    3.00.750E+04.150E-01.125E+06.250E+00.000E+00
    2.00.450E+04.900E-02.240E+04.132E-01.250E+00
    3.00.200E+04.400E-02.000E+00.250E+00.000E+00
    2.00.600E+04.120E-01.400E+04.160E-01.250E+00
    6.00.400E+05.160E+05.300E+01.000E+00.000E+00
    6.00.100E+06.400E+05.300E+01.000E+00.000E+00
    6.00.300E+06.120E+06.300E+01.000E+00.000E+00
    6.00.200E+07.800E+06.300E+01.000E+00.000E+00
    5.00.150E+05.500E+05.121E+04.300E+01.250E+00
    3.00.300E+04.300E-01.250E+05.250E+00.000E+00
    3.00.300E+04.100E-01.750E+05.250E+00.000E+00
    3.00.300E+04.150E-02.500E+06.250E+00.000E+00
    2.00.700E+04.140E-01.350E+04.840E-01.250E+00
    0.0.0917    0.0.0000    0.0.0000    0.0.0917    0.0.0000    0.0.0917
  600.00      50      50                          14      37      14      37
     0.0     0.0-13200.0   120.0
 1.00000 0.00000 0.00000 0.00000 1.00000 0.00000 0.00000 0.00000 1.00000
    1.35  100.00     200                                   1       1
```

Figure B-2.—Input parameters for test site Model B.

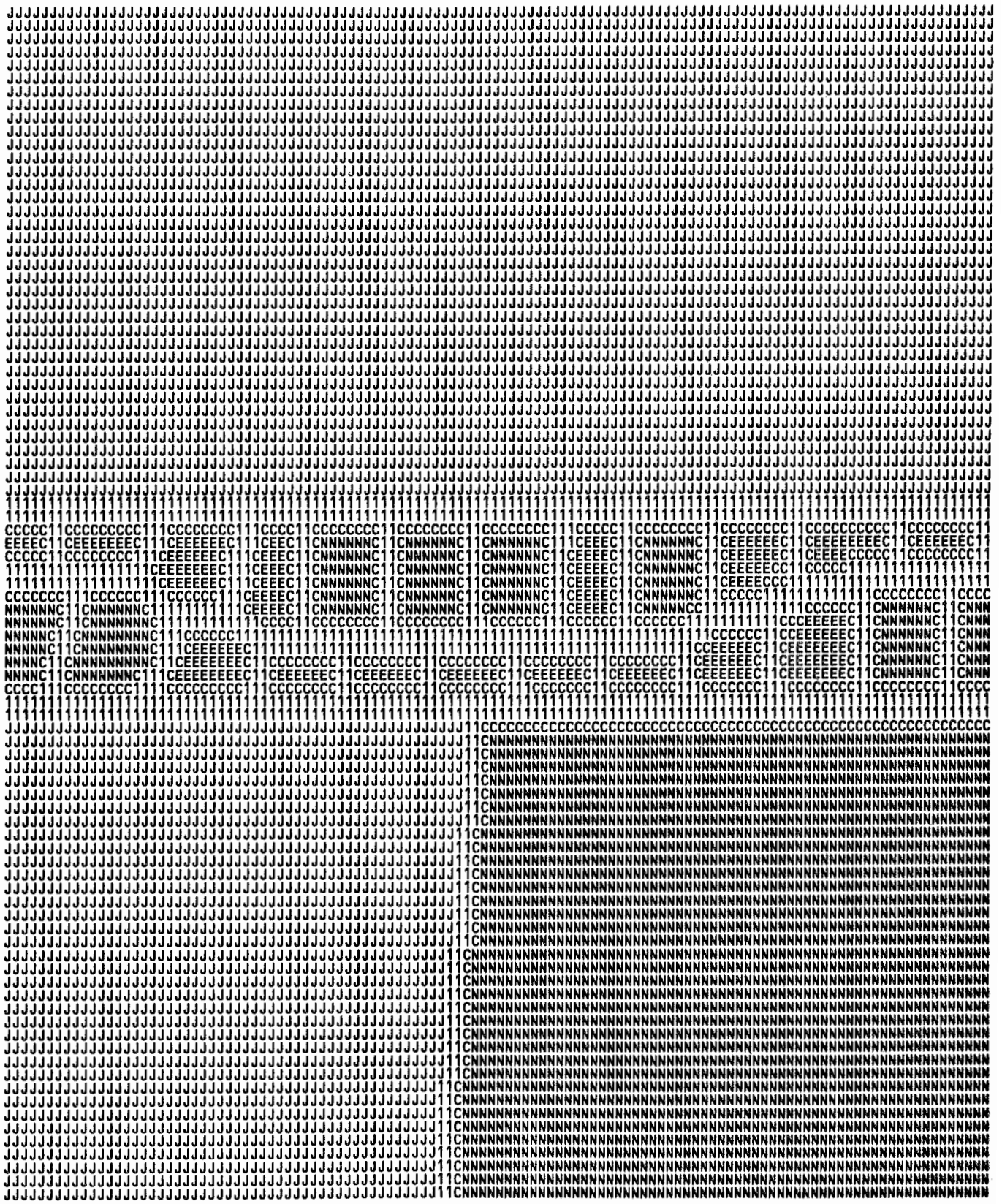

Figure B-3.—Partial fine mesh for test site Models A and B.

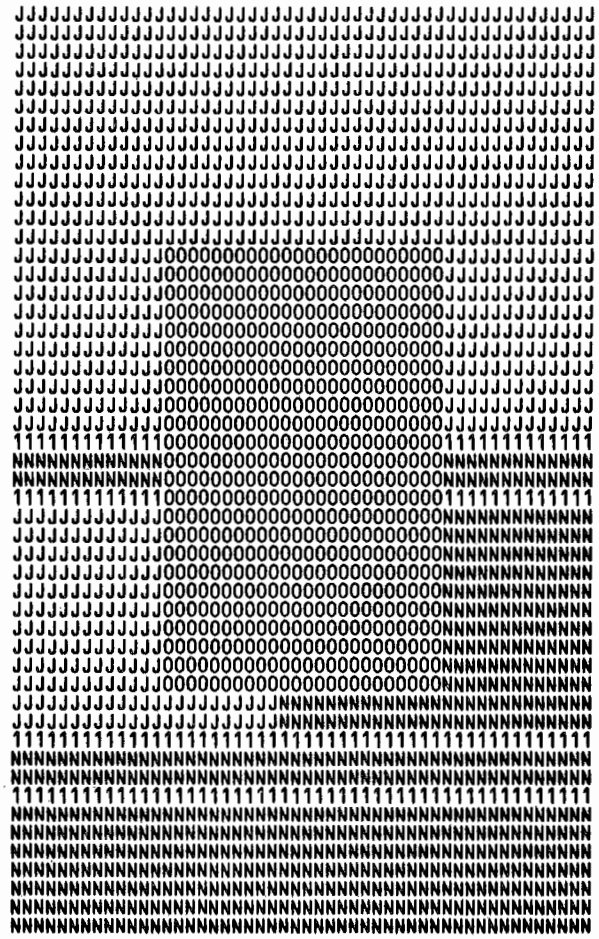

Figure B-4.—Coarse mesh for test site Models A and B.